1974

Surface structures from the interaction of ammonia with tungsten

Douglas Lowell Summers
Iowa State University

Surface structures from the interaction of ammonia with tungsten

by

Douglas Lowell Summers

A Dissertation Submitted to the

Graduate Faculty in Partial Fulfillment of

The Requirements for the Degree of

DOCTOR OF PHILOSOPHY

Department: Chemistry
Major: Physical Chemistry

Approved:

Signature was redacted for privacy.

In Charge of Major Work

Signature was redacted for privacy.

For the Major Department

Signature was redacted for privacy.

For the Graduate College

Iowa State University
Ames, Iowa

1974

TABLE OF CONTENTS

INTRODUCTION

Ultrahigh vacuum techniques developed in the past decade have made it possible to study the interaction of gaseous molecules with atomically clean metal surfaces. The previously discovered catalytic decomposition of ammonia by tungsten metal surfaces has continued to be investigated during this era and is the subject of this dissertation.

In recent years Hansen and associates have used the techniques of flash filament spectroscopy (1) and field electron emission microscopy (2) to characterize the ammonia-tungsten interaction. The primary goal of this research was to obtain information that would lead to an elucidation of the decomposition mechanism. For example, data were obtained concerning rates of decomposition, surface composition, transition state stoichiometries and activation energies. The most recent report from this group was concerned with decomposition rates on single crystal faces (3).

Concurrently, others have investigated this surface interaction on single crystal faces using the technique of low energy electron diffraction (LEED). This technique is qualitatively similar to x-ray diffraction in that it can be used to determine surface structures. The LEED results of ammonia interaction with W(100) (4) and W(112) (5) showed that the structure of the clean crystal face influences considerably the type of surface structure, adsorbate-surface complex, formed

during the decomposition reaction.

The purpose of the investigation reported here was to employ the LEED technique to determine what structures were present on W(100) and W(111) during the steady state decomposition of ammonia as a function of pressure and temperature. Results were obtained at pressures 10^{-6} - 10^{-3} torr. and temperatures 700° - 1100°K. The interaction of molecular nitrogen under similar conditions was also investigated. A qualitative correlation was obtained between the proposed surface structures and species occurring in the kinetic mechanism proposed by McAllister and Hansen (3).

TWO DIMENSIONAL DIFFRACTION AND THE LEED TECHNIQUE

Diffraction from a Two Dimensional Periodic Object

The purpose of the first part of this section will be to derive the equations for two dimensional diffraction using the kinematical or single scattering approximation. This approach is known to work quite well in the case of x-ray diffraction. Though this theory has not had much success in interpretation of LEED results, it has the merit of simplicity and can be used as a starting point for the understanding of more complicated theories. The second part of this section will be to identify two techniques involving dynamical interactions that have been used to interpret LEED data.

Figure 1 shows schematically the various parameters which are important in describing the diffraction from a two dimensional lattice. S is a section of the lattice which in this idealized case is composed of point scatterers of radiation,"atoms", arranged in a perfect two dimensionally periodic manner. T and P are the source of incident radiation and point of observation respectively. Both are of the same order of distance from the origin, O. $\vec{s}, \vec{s}_o$ are the wavevectors of the scattered and incident radiation respectively. There are assumed to be two identical atoms displaced from each other by the vector $\vec{R}_{n,m}$ where one atom is taken to be the origin. The indexing is such that atom (n, m) is the n^{th} atom in the m^{th} unit cell. Formally this is

expressed as:

$$\vec{R}_{n,m} = m_1\vec{a}_1 + m_2\vec{a}_2 + \vec{r}_n \qquad (1)$$

where $\vec{a}_1, \vec{a}_2$ represent the sides of the unit cell and $\vec{r}_n$ is the displacement from the origin of the m_1m_2 cell. For typical diffraction experiments $|\vec{R}_{n,m}| \sim 10^{-8}$ cm. and $\overline{OP}$ or $\overline{TO}$ are ~1 cm. Thus, it is a very good approximation to consider all atoms as being the same distance R from T or P. Also, the incident radiation is taken to be a plane wave.

The amplitude of the scattered radiation at P from atom (n, m) is:

$$\epsilon_{n,m} = \frac{f_n}{R} \cos\left(2\pi\nu t - \frac{2\pi}{\lambda}\phi_{n,m}\right) . \qquad (2)$$

f_n is the magnitude of the radiation scattered by atom (n, m). Generally it will be a function of the wavelength, λ, and scattering angle represented by $(\vec{s} - \vec{s}_o)$. $\phi_{n,m}$ is the phase of the radiation scattered by atom (n, m) with respect to the one at the origin. From Fig. 1 it can be seen that $\phi_{n,m}$ can be written as:

$$\phi_{n,m} = \vec{R}_{n,m} \cdot \vec{s}_o - \vec{R}_{n,m} \cdot \vec{s} = -\vec{R}_{n,m} \cdot (\vec{s} - \vec{s}_o) . \qquad (3)$$

Changing to the complex exponential form the amplitude becomes:

$$\epsilon_{n,m} = \frac{f_n}{R} \exp i\left[2\pi\nu t + \frac{2\pi}{\lambda}(\vec{s} - \vec{s}_o) \cdot \vec{R}_{n,m}\right] \qquad (4)$$

To simplify the remaining calculations the surface region, S, will be assumed to be a parallelogram bounded by sides of lengths $N_1|\vec{a}_1|$ and $N_2|\vec{a}_2|$. The total amplitude at P is now given by summing over all unit cells and all atoms contained in each:

$$\epsilon = \sum_{n,m} \epsilon_{n,m} = \frac{1}{R} \exp 2\pi i \nu t \sum_{n} f_n \exp \frac{2\pi i}{\lambda} (\vec{s} - \vec{s}_o) \cdot \vec{r}_n \qquad (5)$$

$$\times \sum_{m_1=0}^{N_1-1} \exp \frac{2\pi i}{\lambda} (\vec{s} - \vec{s}_o) \cdot \vec{a}_1 m_1 \sum_{m_2=0}^{N_2-1} \exp \frac{2\pi i}{\lambda} (\vec{s} - \vec{s}_o) \cdot a_2 m_2 \ .$$

The first summation is known as the structure amplitude and will be abbreviated as F. It is through this term that the atomic functions, f_n, and the arrangement within each unit cell affect the amplitude of the diffracted beams. The remaining two summations over m_1 and m_2 can be carried out and expressed in closed form. By squaring the total amplitude an expression for the intensity at P is now obtained:

$$\epsilon\epsilon^* = I = \frac{FF^*}{R^2} \times \frac{\sin^2 \frac{\pi}{\lambda} (\vec{s} - \vec{s}_o) \cdot \vec{a}_1 N_1}{\sin^2 \frac{\pi}{\lambda} (\vec{s} - \vec{s}_o) \cdot \vec{a}_1} \times \frac{\sin^2 \frac{\pi}{\lambda} (\vec{s} - \vec{s}_o) \cdot \vec{a}_2 N_2}{\sin^2 \frac{\pi}{\lambda} (\vec{s} - \vec{s}_o) \cdot \vec{a}_2} \ . \qquad (6)$$

For a given lattice structure and fixed wavelength the intensity, I, becomes a function of $(\vec{s} - \vec{s}_o)$. Thus, the function $I(\vec{s} - \vec{s}_o)$ represented by Eq. (6) shows that the most intense scattered radiation will be observed along the direction of $\vec{s}$ that satisfies the following two equations simultaneously:

$$\frac{\pi}{\lambda}(\vec{s}-\vec{s}_o)\cdot\vec{a}_1 = h\pi \qquad (7a)$$

$$\frac{\pi}{\lambda}(\vec{s}-\vec{s}_o)\cdot\vec{a}_2 = k\pi \qquad (7b)$$

where h, k are integers. These are known as the Laue conditions for maximum intensity. The entire diffraction pattern is generated by noting that for fixed λ and $\vec{s}_o$ there will be directions of $\vec{s}$ corresponding to integer pairs (hk) along which intensity maximum will be observed. Equation (6) also predicts that if $N_1 \gg 1$, $N_2 \gg 1$, then nearly all the intensity of each beam will be confined to a very narrow region of space about the maximum. Further information concerning the properties of the function, $I(\vec{s}-\vec{s}_o)$, can be found in most texts that discuss the elementary principles of x-ray diffraction (6).

At this point one has the necessary information to understand the intrinsic difference between two and three dimensional diffraction systems. In three dimensional systems the intensity function, I, would be similar to that of Eq. (6) except there would be an additional $\sin^2(\ )$ term resulting from the additional periodicity that must be specified in 3D systems. This would lead to one more Laue equation of the same form as Eqs. (7a) and (7b) above. In 2D systems only two components of the three dimensional vector $\vec{s}$ are specified by the Laue conditions with the third component being given by the conservation of energy. This results in continuous values for the third component of $\vec{s}$

as a function of $\vec{s}_o$ or λ. Provided λ is small enough the two Laue equations will always yield a value of $\vec{s}$ representing the diffracted beam direction as $\vec{s}_o$ or λ is varied. The experimental observation in a LEED system is that if all other conditions are satisfied a given beam is always observed and moves across the fluorescent screen in a continuous manner as the crystal is rotated or wavelength is varied. For 3D diffraction a beam will only be observed in those rare instances when the orientation of the structure and wavelength are such as to satisfy all three Laue equations. Of course, even in 2D diffraction the FF^* term in the intensity function may cause a given beam to have zero intensity at certain values of λ or $\vec{s}_o$.

The previous derivation of the intensity function was based upon the assumption that one already knew the structure of the two dimensional lattice and had information concerning $F(\lambda, s-s_o)$. The reverse of this is the usual situation in that the intensity of each diffracted beam, I(hk), is used to determine the structure through the application of the appropriate diffraction theory. There are a number of different approaches that can be used within the framework of each theory and no detailed discussion will be given here. However, all methods eventually involve a certain amount of trial and error fitting of the data. In the case of x-ray diffraction a very large number of bulk structures have been determined simply because the well understood equations of

kinematical theory predict the diffracted intensity from most structures with a high degree of accuracy. The scattering of x-ray photons by an individual atom is nearly independent of whether that atom is part of a dilute gas phase or in a close packed periodic bulk structure. However, the interaction of low energy electrons ($\leq$ 1keV.) with periodic structures is not well understood and it appears that kinematical theory may have limited application in LEED. Most intensity functions in LEED, I(hk), exhibit much more structure than the Bragg peaks predicted by kinematical calculations. The reason for the complicated dependence of the I(hk) function parameters is mainly due to the very large scattering cross sections ($\sim 10^{-16} cm^2$) of most atoms for low energy electrons. This leads to a high probability of multiple scattering and dynamical interactions that must be accounted for before determining surface structures. The following will be a brief description of two techniques that have been used to calculate LEED intensities. For further details one is advised to consult recent reviews of LEED results (7, 8, 9).

Basically there have evolved two approaches to the calculation of LEED intensities. One is the band matching technique which is derived from well developed methods of band structure calculations. Using this method one begins with the wave equation and solves for the internal solutions inside the solid at given energy and surface momentum component of the incident beam. The second step is to match the

internal solution and its surface normal derivative to external solutions in the vacuum. Another technique has been to solve the wave equation by an integral solution that involves a Green's function. In this approach the scattering factors for the lattice atoms (ion cores) can be determined independently and then used as input into the main program for intensity calculations.

Hirabayashi and Takeishi (10) performed one of the first calculations using a method similar to the band matching approach. They calculated the intensity of the specular beam from a graphite surface. The approach was restricted in that a self-consistent solution was not obtained, instead the two beam approximation was used. This approximation only allows for an incident beam and one diffracted beam with the incident beam amplitude being much greater than the diffracted amplitude. Calculated intensities agreed fairly well with experimental results for energies >100 eV. but very poorly at lower energies. The results of their calculations indicated that a more realistic approach would involve a self-consistent solution of the wave equation.

E. G. McRae (11) was the first to attempt a self-consistent calculation. His starting equations were those derived by Lax (12) many years earlier. The technique was to use Green's integral method for solving the wave equation. The self-consistent nature of the calculations is illustrated by two facts. First, the amplitude of the wave field at any

point in space is the superposition of the incident field from an external source and the sum of all waves scattered by the lattice. Second, the field amplitude incident on any one lattice atom is equal to the total wave field minus the field emitted by the atom being considered. Thus, the amplitude incident on any one atom is a function of the fields emitted by all other atoms.

Using this method the form of the solution is:

$$\Psi(R) = \Psi^{O}(R) - \sum_{s} \int G(R, R')T(R', R_s)\,\Psi^{s}(R')dR' \qquad (8a)$$

$$\Psi^{t}(R) = \Psi^{O}(R) - \sum_{s \neq t} \int G(R, R')T(R', R_s)\,\Psi^{s}(R')dR' \qquad (8b)$$

where: $\Psi(R)$ is the field amplitude at point R, $\Psi^{O}(R)$ is the external incident beam amplitude, $G(R, R')$ is the appropriate Green's function and $T(R', R_s)\,\Psi^{s}(R')$ represents the effect of the incident wave field upon the s^{th} atom. $\Psi^{s}(R)$ is the effective field incident on the s^{th} atom. A logical consequence of using this approach is that all orders of scattering are taken into account.

The intensity of the specular beam from a simple cubic lattice of isotropic scatterers was calculated. As expected the results showed the occurrence of the ordinary Bragg peaks. In addition secondary Bragg peaks were predicted. These result from the incident radiation being scattered into some intermediate beam in the lattice and then undergoing a second scattering into a beam traveling away from the

surface into the vacuum. It was also shown that as the scattering cross section of the atoms was reduced the intensity due to all phenomena other than Bragg diffraction decreased very rapidly. Thus, the kinematical approximation is obtained as a limiting condition using this approach.

The previous discussion was limited to two specific examples in order to show the manner in which intensity calculations have progressed beyond the kinematical solution to the wave equation. There have been further contributions to this area and one should consult current LEED literature for additional information. Unfortunately, very few attempts to calculate the surface structure due to light gas adsorption have been reported. Generally most results have only been concerned with determining the intensities from clean surfaces. Calculations directed to this area of surface interactions would certainly be helpful to those interested in the chemistry of surface systems.

LEED Nomenclature

For LEED to develop into an exact science such as x-ray diffraction a system for describing surface structures will be required. Since at present it is not possible to completely determine surface structures from LEED data, a comprehensive nomenclature that describes all the spatial symmetries cannot be developed. Of course, one could argue that the space group notation used in three dimensional analysis adequately describes every possible structure; thus, this

convention should be used in LEED structure analysis. There are two reasons why this has not been the case. First, the present qualitative knowledge of most surface structures would probably result in different authors using different symbols to describe the same structure especially since very little is known about possible symmetry operations normal to the surface. Second, and probably most important, surface scientists are generally interested in the relationship between a given surface structure and the substrate or original surface from which it may have been formed. Space group notation would need to be modified to show that such a relationship may exist.

The purpose of this section is not to introduce any new terminology since the existing nomenclature conventions adequately describe what is known about most surface structures. Instead, it is intended to give the reader a basic understanding of the meaning of symbols that are currently in popular use in LEED literature and that will be used in this dissertation. A more illustrative approach can be found in a recent compilation of LEED results (13).

In the current literature there is a certain amount of ambiguity as to the meanings of the terms "surface" and "substrate". It was initially proposed (14) that the term "substrate" be used to describe only that portion of the bulk material that strictly maintained periodicity in the direction normal to the surface. "Selvedge" was to be that region

between the substrate and surface plane. These definitions have not been widely accepted. Generally the surface is the very first or possibly first and second atomic planes which may be comprised of a structure different from the substrate upon which it rests. In this dissertation the term "surface structure" will apply to only the top atomic layer of metal atoms which may also contain light adsorbate atoms and generally will have a two dimensional structure different from that of a parallel plane in the bulk. "Substrate" is the second and successive layers of metal atoms and will be assumed to have a 2D structure identical to a parallel bulk plane.

The notation of Wood (14) and Lander (15) has generally proven sufficient in describing surface structures and the relationship that may exist between the surface and substrate structures. The labeling of a structure begins by expressing the planar vectors $\vec{a}_s, \vec{b}_s$ of the surface structure in terms of the substrate vectors $\vec{a}, \vec{b}$:

$$\vec{a}_s = m\vec{a} \qquad \vec{b}_s = n\vec{b} \quad . \tag{9}$$

Using this notation it can be seen there is a coincidence between the surface and substrate lattice points of $m|\vec{a}|$ spacings along the direction of $\vec{a}$ and $n|\vec{b}|$ spacings along the $\vec{b}$ direction. This results in a system (superstructure) periodicity of (m x n) referred to the periodicity of the substrate. It is this periodicity which determines the diffraction angles for allowed beams and not the periodicity of the surface or substrate

structure alone. If the surface structure is rotated with respect to the substrate then this is symbolized by adding an "R" followed by the angle of rotation. For example, a (2 x 1) R-30° notation would describe a structure whose unit cell vectors $\vec{a}_s, \vec{b}_s$ were rotated 30° with respect to $\vec{a}, \vec{b}$ respectively. The length of $\vec{a}_s$ would now equal two of the substrate spacings along the direction of $\vec{a}_s$ which in general is not equal to the substrate spacing along $\vec{a}$. Similarly, $\vec{b}_s$ would have a length of one substrate spacing along the direction of $\vec{b}_s$. These definitions in the case of a rotated structure would still describe the superstructure periodicity. However, the notation is somewhat awkward especially if the interaxial angle between the surface unit vectors does not equal that between the substrate vectors.

To eliminate this problem Park and Madden (16) have generalized the (m x n) notation such that a (2 x 2) matrix is used to express the relationship between the surface and substrate structures. In their system $\vec{a}_s$ and $\vec{b}_s$ are each defined in terms of $\vec{a}$ and $\vec{b}$:

$$\begin{aligned} \vec{a}_s &= n_{11}\vec{a} + n_{12}\vec{b} \\ \vec{b}_s &= n_{21}\vec{a} + n_{22}\vec{b} \end{aligned} = \begin{pmatrix} n_{11} & n_{12} \\ n_{21} & n_{22} \end{pmatrix} \begin{pmatrix} \vec{a} \\ \vec{b} \end{pmatrix} . \qquad (10)$$

It is the matrix, (N), which is used to symbolize the periodicity of the system. For surface and substrate unit vectors which are colinear the obvious equivalence between the (m x n) symbol and the matrix notation is:

$$(m \times n) = \begin{pmatrix} m & 0 \\ 0 & n \end{pmatrix} \quad . \qquad (11)$$

For these simple cases the $(m \times n)$ notation is more compact and it is generally used in preference to the matrix form. However, for rotated surface structures the matrix notation is the least ambiguous and should be used even though some of the n's may be quite large.

In addition to the periodicity notation discussed above other symbols are generally present to further classify the particular structure being considered. The clean surface orientation is usually identified and in special cases the chemical symbol and fractional coverage of an adsorbate are denoted where adsorption has resulted in a new surface structure. Therefore, the following sequence of information may be encountered in a complete structure classification:

1) The chemical symbol of the material whose surface is being investigated and its clean surface orientation.

2) The complete (N) matrix or $(m \times n)$ symbol to denote the periodicity.

3) The chemical symbol of the adsorbed species responsible for the new surface structure.

4) The fractional coverage of the adsorbate denoted in 3).

Examples of this convention can be illustrated by presenting the notation used to describe three of the structures that occur when oxygen

adsorbs on Ni(110) at 1/3, 1/2 and 2/3 coverage respectively (17). They are: Ni(110) -$\begin{pmatrix} 3 & 0 \\ 0 & 1 \end{pmatrix}$-0-[1/3], Ni(110) -$\begin{pmatrix} 2 & 0 \\ 0 & 1 \end{pmatrix}$-0-[1/2] and Ni(110)-$\begin{pmatrix} 3 & 0 \\ 0 & 1 \end{pmatrix}$-0-[2/3]. These can also be described by the (m x n) notation as (3 x 1), (2 x 1) and (3 x 1) respectively. If in the (m x n) notation it appears convenient to define a centered cell then the letter "C" precedes the symbol such as C(2 x 2) which is a commonly encountered structure in LEED.

There are known to be some materials whose apparently clean surfaces undergo a reconstruction or relaxation to create a surface structure different from that of a parallel plane in the bulk. In these special cases symbols for 3) and 4) above would be omitted. An example of this type would be the (100) face of clean platinum which appears as a (5 x 1) structure (18). Using the above convention this would be written as Pt(100) - (5 x 1).

Pattern Indexing

A closely related subject to nomenclature is that of diffraction pattern indexing. For LEED systems this is a relatively simple operation since one usually obtains a pattern from the clean surface of known geometry and then compares this to any pattern resulting from a structural transformation to obtain diffraction angles and unit spacings. Analogous to x-ray diffraction the LEED beams are labeled by the Miller indices. Since LEED is nearly a two dimensional diffraction system,

only two indices are required for each beam; these are the Miller indices of the rows of atoms in the surface plane.

Once a coordinate system and unit cell have been chosen for the structure the Miller indices, hk, determine the direction and spacing between parallel rows. For the general two dimensional system the spacing, d_{hk}, among the set of parallel rows denoted by {hk} is:

$$\left(\frac{\sin\gamma}{d_{hk}}\right)^2 = \left(\frac{h}{a}\right)^2 + \left(\frac{k}{b}\right)^2 - \frac{2hk\cos\gamma}{ab} \qquad (12)$$

where a, b are the lengths of the unit cell sides and γ is the a, b inter-axial angle. The indices hk are the same integers that occur in the Laue equations (Eqs. 7a and 7b). By measuring the angle of diffraction for a given beam from the pattern and knowing the wavelength ($\lambda = \frac{12.25}{\sqrt{eV}}$A) one can calculate the interrow spacing using the Laue equations.

If a and b are identified with the unit cell of the clean surface then quite often an experiment will lead to a new structure with unit cell dimensions equal to some integral multiple of a and b. This transformation will give rise to new beams that are positioned between those from the original surface. If this is the case, the normal convention has been to assign fractional order indices to the new beams. A given structure denoted by (m x n) will produce fractional order beams with indices $\left(\frac{h}{m}, \frac{k}{n}\right)$. Of course, certain of these beams may not be observed due to symmetry extinction conditions. For example, a (2 x 2) structure will result in new beams $\left(\frac{h}{2}, \frac{k}{2}\right)$ for h, k equal to any integers; a C(2 x 2)

will give half order beams also, but only for those beams in which h+k equals an even integer.

Domains

The domain character of surface structures has proven to be one of the more interesting aspects of LEED investigations. Previous to LEED it was not a widely accepted idea that surface structures could possess a degree of long range ordering. The following discussion will be concerned with a qualitative definition of the term "domain" as it is commonly used in LEED literature and the effect of domain structure on the observed diffraction patterns.

A domain can be thought of as a region of the surface, the interior of which is a homogeneous structure. The boundary of such a region is generally not well-defined from the experimental point of view. The domain tends to be of a very irregular shape with an increasing number of imperfections as one proceeds outward from its interior.

There are two different aspects of domain structure to be considered in surface investigations. The first of these is the domain character of the clean unreacted surface (substrate). Domains of this type are separated from one another by random imperfections such as cracks, pits, dislocations, etc. which have been induced to a large degree by the sample surface preparation technique. They are analogous to the commonly encountered mosaic structure of x-ray

diffraction. Since there is no coherence or definite phase relationship between their placements, the diffracted intensity from each domain independently contributes to the observed diffraction pattern. LEED patterns appear to be insensitive to this type of domain structure. Surfaces that are very rough macroscopically can still give well-defined diffraction patterns.

The work of Park and associates has been concerned with the effects of domain structure on beam profiles and intensity functions (16, 19-22). In experiments on Ni and Pd surfaces it was concluded that a lower limit of substrate domain diameter was $\sim 10^2$ Å (16, 19). This limit is determined by the resolution of the electron optics. Beamwidths and intensity distributions were investigated with respect to bombarding these surfaces with 400-500 eV. argon ions. Although ion bombardment leads to beam broadening the domain size is not significantly altered. Instead, it was concluded that embedded ions distort the perfect lattice arrangement within each domain.

The effect of steps on beam intensity distribution has also been studied by this group (20-22). Each domain heretofore assumed to have a perfect planar structure most likely has numerous steps within its boundaries. On most surfaces the steps occur at random displacements in the surface plane. However, in the direction normal to the surface steps are not considered as a random imperfection since the height of

each step is some integral multiple of the interplanar spacing between parallel planes. With respect to the diffracted beams there are peaks in the I(E) distribution associated with steps. It was an interesting result that ion bombardment did not appreciably effect these peaks while significantly altering the normal Laue intensity peaks (20).

The second type of domain structure to be considered is that which occurs as the result of the clean surface undergoing a chemical reaction. Such an example would be the chemisorption of hydrogen on a W(100) surface. Domain structure in this case can occur because of the high probability that a surface structure was nucleated at more than one site within a single domain of the substrate. This is not to be confused with mosaic structure since a definite phase relationship can exist between surface domain placements. If there are a number of energetically equivalent ways the surface structure can be placed on the substrate, generally all orientations will be present to the same extent. If more than one of these is present on a single domain of the substrate and within the coherence region of the optics, interference effects should cause a systematic variation in the beam intensities. If a single domain of the substrate accommodates only one surface structure domain then no interference occurs and the intensity from each domain contributes independently to the total diffraction pattern. One example of the way in which domain structure can influence the

diffraction pattern will be given next.

A common occurrence in LEED is that surface structures formed by reaction of the original surface appear to have the same two dimensional rotational symmetry as the original surface as judged from the diffraction patterns. This necessarily leads to confusion in some cases since these patterns can also be explained by noting that multiple orientations of domains with lower symmetry can produce the same result. For example, a (2 x 1) structure which has twofold rotational symmetry could have two energetically equivalent placements on a substrate which has fourfold symmetry. This case occurs during the high temperature interaction of oxygen with W(100) (23). In this system the diffraction pattern displays half order beams with indices $(\frac{h}{2}, k)$ and $(h, \frac{k}{2})$ with h, k equal to any integer. A (2 x 2) structure would result in the same beams, but in addition beams with indices $(\frac{h}{2}, \frac{k}{2})$ would be present. The absence of the $(\frac{h}{2}, \frac{k}{2})$ beams in the pattern is interpreted to mean that the half order spots are due to two equivalent orientations of the (2 x 1) structure on the fourfold (100) substrate. Half of the domains result in the $(\frac{h}{2}, k)$ beams and the other half rotated at 90° give the $(h, \frac{k}{2})$ beams. The above example was one in which the distinction between structures could be made on the basis of symmetry extinction conditions. However, there are cases in which this is not possible and one must always be prepared to allow for possible rotational degeneracies when interpreting complex patterns.

REVIEW OF PREVIOUS RESEARCH ON THE INTERACTION OF NH_3, N_2 AND H_2 WITH TUNGSTEN SURFACES

Introduction

The purpose of this review will be to present and discuss only those results obtained during the last decade using ultra high vacuum techniques to investigate the ammonia/tungsten interaction. Principally the techniques have been thermal desorption spectroscopy (TDS), field electron emission (FEM), and LEED. A number of reviews have been published concerning the earlier research on this system and one should consult them if further background information is needed (24-28). During the course of recent research the related systems, N_2/W and H_2/W, have been investigated on polycrystalline wires and single crystal faces. For the purpose of this dissertation H_2 and N_2 results on single crystal faces will be presented. A polycrystalline surface is ill suited for a discussion of adsorbate structures, but it appears that in one instance there exists a relationship between the results on single face and polycrystalline surfaces with respect to the NH_3 interaction with tungsten. Initially, only results and conclusions of individual investigations will be presented on the H_2, N_2 and NH_3/W systems and will be followed by a critical discussion.

Hydrogen on Single Crystal Faces

The adsorption of hydrogen on W(100) has been investigated extensively (29-33) with some results also obtained on the (111) (34), (110) (34-36), and (112) (5, 37, 38). Generally most of the experiments were performed in systems with hydrogen partial pressures $\sim 10^{-8}$ torr. and sample temperatures $\sim 300°$K. The following will be a summary of results on the (100) surface followed by brief comments on results obtained on other faces as they relate to the (100) face.

In an early LEED investigation of the H_2/W(100) system (29) it was found that initial adsorption at ~300°K resulted in a C(2 x 2) pattern. This pattern attained a maximum intensity at a surface coverage of $\sim 5 \times 10^{14}$ atoms/cm^2. Further adsorption caused the 1/2 order beams to split and gradually decrease intensity until the surface was saturated and a (1 x 1) pattern was observed. Measurement of the saturation coverage showed it to be $\sim 2 \times 10^{15}$ atoms/cm^2. It was concluded that the C(2 x 2) was due to a half monolayer of dissociated hydrogen and that the (1 x 1) was the result of single atoms bonded in every bridge position on the (100) surface. The bonding energy on this surface was measured by observing the temperature interval of desorption in TDS experiments (30). Two surface states, designated β_1 and β_2, were observed to desorb at maximum rates at ~450° and ~550°K respectively. The corresponding activation energies of

desorption, E_d, were 26.3 and 32.3 kcal./mole. Determination of the partial coverages in each of these states gave the following results: $n_{\beta_1} = 1 \times 10^{15}$ atoms/cm^2 and $n_{\beta_2} = 5 \times 10^{14}$ atoms/cm^2. Thus, the conclusion was that β_2-H was the state responsible for the C(2 x 2) structure. However, this was reinterpreted later after LEED and coverage experiments had been carried out simultaneously in the same vacuum system (32). Results in this system showed that the C(2 x 2) pattern had a maximum intensity at $\sim .15$ x saturation coverage. Using the previously determined value of 1.5×10^{15} atoms/cm^2 as the saturation density it was obvious that the maximum intensity of C(2 x 2)-H did not correspond to a half monolayer of hydrogen atoms. The authors proposed a model in which a certain amount of hydrogen was always present on the surface and dissolved into the bulk at higher temperatures instead of desorbing. The proposed model would have a saturation coverage of 2×10^{15} atoms/cm^2 all of which could not be desorbed at high temperatures. A very recent investigation (33) has shown the desorbable coverage to be 2×10^{15} atoms/cm^2.

On (110), (112) and (111) surface high energy surface states exist corresponding to the β states on (100). The (111) face produces three such states due to adsorption at 300°K (34). However, there is some puzzlement as to why these high binding energy states do not produce any ordered LEED patterns other than (1 x 1)'s. This may be

the result of the surface states having a high degree of mobility with very little correlation between hydrogen atom positions. However, this will probably not be resolved until substantial progress is made in the understanding of the LEED process.

Nitrogen on Single Crystal Faces

One of the earliest investigations of nitrogen interaction with tungsten single crystal planes provided information about the energetics of bonding and work function changes due to adsorption (39). (100), (110) and (111) surfaces were studied. The results indicated that at least one high energy state, β, was formed on the (100) and (111) surfaces at 300°K with E_d = 75 - 80 kcal/mole and that nitrogen does not adsorb on the (110) at this temperature. The work function changes were found to be: $\Delta\phi_{(100)} = -0.4$eV, $\Delta\phi_{(111)} = 0.15$eV and $\Delta\phi_{(110)} = 0.0$eV. The β states desorbed via second order kinetics and were assumed to be atomic. A LEED investigation of the (100) showed that β-N had a C(2x2) structure (40) and later TDS experiments indicated a coverage of 5×10^{14} atoms/cm^2 for this state (41). In addition it was shown that a second β state can be formed on (100) that desorbs via first order kinetics only a few hundred degrees below the initially discovered β state. These two states, labeled β_1 and β_2, desorb with activation energies, E_d = 49 kcal/mole for β_1 and 73.5 kcal/mole for β_2. It has been reported that an atomic β state can be formed on the

(110) plane (42). E_d for this state was 79 kcal/mole, but its formation takes place at a very low rate with an initial sticking coefficient of 0.005 and saturation coverage of $\sim 1.8 \times 10^{14}$ atoms/cm^2. However, a recent investigation using a molecular beam method showed no adsorption occurred on (110) in agreement with the initial study of this interaction (43).

LEED and $\Delta\phi$ measurements have recently been reported on the (210) and (310) surfaces (44). These planes interact with nitrogen in a manner similar to (100). Adsorption at 300°K resulted in double spaced structures which desorbed in a single high temperature peak. Unlike (100), adsorption results in a work function increase on both planes. The values of these increases are: $\Delta\phi_{(310)} = 0.20$eV and $\Delta\phi_{(210)} = 0.27$ eV.

Ammonia on Polycrystalline Wires

From results obtained using a field electron microscope Dawson and Hansen (2) proposed that in the temperature range of catalytic interest, 900° - 1100°K, the tungsten surface would be substantially covered with a hydrogenated surface nitride. Its structure was proposed to be:

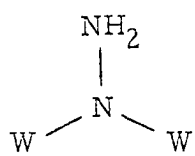

and its decomposition was the rate limiting step of the overall reaction. Since a hydrogen isotope effect had been found previously (45, 46), the above structure appeared reasonable.

TDS experiments by Matsushita and Hansen (1) on a polycrystalline wire showed that when ammonia interacted at 300° K substantially all hydrogen could be desorbed from the surface by ~ 900° K. Also, nitrogen adsorption due to ammonia decomposition resulted in a nitride state that could not be formed by the adsorption of molecular nitrogen. The surface stoichiometry of this state, x, at full population was nearly WN. This nitride desorbed in the range ~900° - 1100° K via second order kinetics with E_d = 49 kcal/mole. The rate of desorption of this state was shown to agree reasonably with decomposition rates obtained by others. The nitride contained essentially no hydrogen and its existence was at variance with the earlier FEM results.

Further investigation by Peng and Dawson (47) on a polycrystalline wire confirmed that a hydrogenated nitride could exist at high temperatures if: 1) ammonia was adsorbed at relatively high temperatures, 700° - 1000° K, and 2) the surface had been dosed with relatively large amounts of ammonia, 10^4 - 10^6 L. These experiments showed that this nitride state, η, desorbed at a slightly lower temperature than WN and was formally represented to have the stoichiometry of W_2N_3H. Thus the decomposition of this hydrogenated species was proposed as the rate

limiting step in the total reaction. Kinetic parameters were not presented to further substantiate this conclusion.

Ammonia on Single Crystal Faces

The adsorption and decomposition of ammonia have been investigated on the (100) (4) and (211) (5) surfaces using LEED and TDS methods. These experiments showed that both surfaces have some similarities with respect to ammonia interaction. The initial adsorption at 300°K produced no new features in the LEED patterns other than an increase in background intensity and the work function of both surfaces decreased ~1.0eV due to initial adsorption. When heated above ~1100°K both surfaces desorb nitrogen and hydrogen simultaneously in a single pressure burst with a N:H ratio of 1:2. However, there are differences with respect to the LEED results when the surfaces are heated above ~800°K.

If the (100) is saturated with NH_3 at 300°K and heated to ~800°K a C(2x2) pattern is observed. Further heating to 1400° causes the C(2x2) to disappear and only the (1x1) of the clean surface remains. A single pressure burst occurs during heating above 800° and mass analysis indicates a stoichiometry of NH_2 in this peak. Thus, heating to 800°K results in a surface stoichiometry of W_2NH_2 with a C(2x2) structure. A more dense nitride state can be obtained by repeated adsorption at 300°K and heating to ~800°. Complete population of this

state results in a (1 x 1) structure of stoichiometry WNH_2. The work function changes for the two nitrides are: $\Delta\phi_{W_2NH_2}$ = -0.4eV and $\Delta\phi_{WNH_2}$ = 0.0eV. WNH_2 can also be formed by allowing ammonia to adsorb at ~800°K.

Heating the ammonia saturated (211) surface to ~750°K results in a C(4 x 2) structure. The further heating to ~1400°K gives rise to a single pressure burst of NH_2 stoichiometry. However, if the surface is heated in incremental steps in the interval 800° - 1050°K a variety of LEED patterns is observed. The first of these is the well-ordered C(4 x 2) and the last is a C(10 x 2). This series of patterns has been interpreted as being due to the continuous expansion of an NH_2 adsorbed layer along the close packed $(\bar{1}\bar{1}1)$ direction. Above 1050° the patterns are similar to those observed in the N_2/W(211) system (48). Unlike (100), the repeated dosing at 300° and heating to 800° does not result in new surface structures being formed with respect to single dosing at 300° and heating. Instead, this treatment causes each of the C(4 x 2) - C(10 x 2) patterns to increase total sharpness and intensity. This was interpreted as the formation and growth of NH_2 "islands" with increasing coverage and not to a creation of a new surface state. All of the NH_2 structures had $\Delta\phi$ values ~ 0.0eV.

McAllister and Hansen have recently measured the ammonia decomposition rates on (100), (110) and (111) faces (3). These

experiments were carried out at temperatures 800° - 970° K and ammonia pressures $0.5 - 100 \times 10^{-3}$ torr. The proposed mechanism involved the degradation of $W_2N_3H_2$ as the rate limiting step. Also, the activity of the (111) face was substantially greater than that of the (100) or (110) faces. Activation energies were of the order of 20 - 30 kcal/mole on all surfaces.

Discussion

The preceding was intended only to present experimental results and conclusions of the individual investigators. The following discussion will be a summary and critical comments concerning the interpretation of these results and their relationship to the catalyzed decomposition of ammonia on tungsten.

N_2 and H_2 require very little activation energy to adsorb dissociatively on most crystal faces of tungsten. These atomic states, β-H and β-N, are quite stable and will desorb at appreciable rates only at elevated temperatures ~500° and ~1200° K respectively. The most stable β-N states which can be formed by ammonia or nitrogen adsorption are inactive in the decomposition reaction at 900° - 1100° K due to their very low desorption rates at these temperatures.

Despite the number of investigations that have been reported it is still not certain what is the composition or structure of the surface

during steady state ammonia decomposition. For W(100) and polycrystalline wires it appears that at least two and possibly three nitride states can exist during reaction depending upon the pressure and temperature conditions. Some controversy exists concerning the occurrence of bound hydrogen in these surface states and this will be discussed after comments pertaining to the composition and structure of the nitride states.

Estrup and Anderson (4) isolated what they claimed to be W_2NH_2 on (100). The LEED structure, C(2x2), and temperature of desorption ~1200°K have caused others to claim that this state was actually the β-N state that can be formed by N_2 adsorption and has a surface stoichiometry of W_2N (49). In their experiments on (100) adsorption took place at ~300°K and $\sim 10^{-8}$ torr. Matsushita and Hansen (1) showed that under such conditions essentially all the hydrogen was desorbed from a wire by ~900°K. If the C(2x2) was actually W_2N then this surface state has very little to do with NH_3 decomposition at 900° - 1100°K due to its extremely low desorption rate at these temperatures.

Exposing the tungsten surface to ammonia can also result in a WN surface state being formed. In their LEED investigation Estrup and Anderson (4) claimed to have isolated WNH_2 which had a (1x1) structure and resulted in two nitrogen desorption peaks. Discounting

the presence of hydrogen the same state has been found on polycrystalline wires (1, 47). Only ~50 kcal/mole is required initially to desorb nitrogen from this structure, however its formation from molecular nitrogen can only be accomplished by activated molecules (49) or very high exposure, $\sim 10^3$ L, of unactivated molecules (41). It is reasonable to expect that the $(\beta_1 + \beta_2)$-N state formed on W(100) from N_2 in TDS experiments is identical to WN formed by ammonia interaction. The TDS results did not necessarily show a stoichiometry of WN, but the E_d of 50 kcal/mole is a good indication that both states are identical. The LEED investigation of (100) also showed that partial population of WN results in a 1/6 order structure.

A third state, W_2N_3H, can also be formed by interaction at relatively high exposures, $10^4 - 10^6$L, of ammonia at moderate temperatures 700° - 900°K (47). Initially this species was isolated on a polycrystalline wire, but the recent kinetic results of McAllister and Hansen (3) support the existence of a similar state, $W_2N_3H_2$, on W(100), (110) and (111). However, it is probably present only at relatively high pressures, $\gtrsim 10^{-3}$ torr., during steady state reaction. Presently there is no further reported evidence for this state, but the determination of its structure will most likely receive attention in future investigations.

As implied by this discussion the controversy over surface hydrogen is still unsettled. Although the investigations on (100) and

(112) showed the presence of bound hydrogen at high temperatures this may have been an artefact of the experimental system such as desorption from support leads. Experiments with small diameter wires are not prone to such systematic errors and it is found that hydrogen desorption is essentially complete by 900°K (1). This is the case when adsorption takes place near 300°K. The results of Peng and Dawson (47) on wires and McAllister and Hansen (3) show strong evidence for bound hydrogen if interaction takes place at higher temperatures, 700° - 900°K.

The question of hydrogen presence would be somewhat inconsequential if it were not for the fact that kinetic measurements using NH_3 and ND_3 have shown that these species react at different rates. Very early research on wires (45, 46) and recent experiments on single crystal faces (3) have confirmed this result. One interpretation of this isotope effect is that ND_3 and NH_3 have different dissociation equilibrium values and this would lead to differences in the surface concentrations for their dissociation products. This interpretation would be favored by those who believe that nitrogen desorption is the rate limiting step. Alternatively, the effect could be explained by proposing that the transition state of the rate limiting step contains hydrogen bonds. This explanation in terms of a kinetic effect contradicts the idea of nitrogen desorption being rate limiting.

In principle the LEED technique could resolve this question of hydrogen content, however the understanding of the LEED process will need to make considerable progress before it can be used to determine absolute surface structures.

EXPERIMENTAL

Purpose of Experiments

The object of the experimental procedure was to determine the surface structure(s) that are present on single crystal faces of tungsten when ammonia catalytically decomposes in a steady state reaction. Previous results had indicated possible structural dependencies upon pressures and temperatures of interaction. These experiments were performed at ammonia pressures = 10^{-6} - 10^{-3} torr. and temperatures = 700° - 1100° K. It was also desirable to determine the structures resulting from the steady state interaction of nitrogen. Thermal flash desorption analysis of nitrogen and hydrogen from W(100) and (111) were performed to check characteristics of surfaces in this system against those of previous investigators outside this laboratory.

Experimental System

The vacuum system in which all experiments were performed is shown in Fig. 2. The attainment of laboratory ultra high vacuums, $\sim 10^{-10}$ torr., has become a routine procedure in the past decade and the system used in this investigation incorporates a number of components that are standard on such systems. Continual pumping is obtained by a 20 l/sec. ion pump (Ultek D-1). During bake-out or experiments requiring pressures greater than $\sim 10^{-5}$ torr. the ion pump is turned

off and a liquid nitrogen trapped mercury diffusion pump is connected to the system via a 1" diameter metal seal valve. The top side of the system which housed the LEED electron optics (PHI No. 10-180) is essentially a $5\frac{1}{2}$" diameter x 12" glass cylinder that has a glass-kovar seal at one end. The kovar seal is welded to an 8" flange which has a large circle cut out of its center and allows the electron optics to be installed through its opening.

There are four large diameter, 38 mm, side arms sealed to the cylinder which connect to the sample holder dewar assembly, ion gauge, mass spectrometer and ion pump. A small diameter tube is attached for the purpose of leaking in sample gases from the gas storage manifold through a Granville-Phillips metal seal "A" valve. The fluorescent screen of the optics is viewed through a glass circle sealed to the front of the main cylinder.

The sample is a disc, .015" x .25", cut from a tungsten single crystal rod to expose either a (100) or (111) plane at its surface. Each sample disc was cleaned by high temperature heating for a few days followed by oxygen treatment at elevated temperatures.

The disc is suspended in front of the electron optics by use of the holder assembly. The details of this assembly are shown in Fig. 3. An .018" diameter tungsten wire is spot welded to the sample and welded to the heavier support leads of a glass press seal. The leads of the

press seal pass through the top of the system and allow for external electrical connections. The holder assembly also allows for the temperature of the crystal to be monitored by a W/Re5% - W/Re26% thermocouple. Each thermocouple wire is continuous from the sample to the external reference junction. Thus, no dissimilar metal-metal contacts are present internally in the thermocouple circuit which averts errors in temperature measurement due to temperature gradients along the wires.

The sample is heated by bombardment with a nominal current, 1-100 ma., of 400 eV electrons which are emitted from a thoriated Ir filament suspended directly behind the sample. This technique allows the sample to be heated to ~2500° K for the purpose of cleaning. The steady state temperature of the crystal is maintained by establishing a constant emission current from filament to sample. An external electronic regulator performs this function by controlling the filament heating current.

Procedure

For thermal desorption experiments the initial step was to clean the sample by maintaining it at ~2000° K and pressure ~10^{-9} torr. for 10 minutes. The sample then cooled for 15 minutes and a high temperature flash, ~2500° K was used to desorb any material adsorbed during the cooling period. After flashing the crystal was allowed to cool to

$\sim$ 750° (100) $\sim$ 600° (111), then dosing of the sample gas, H_2 or N_2, was begun and continued for 5 minutes. During this time the sample cooled to 450° (100), 400° (111). The leak of sample gas was then stopped and the crystal heated at a rate to permit sufficient resolution of the desorption curves, desorption rate vs. temperature, in the temperature intervals of significant gas desorption.

The initial step in the ammonia steady state experiments was to establish a predetermined steady state ammonia pressure in the system. This was done by monitoring the m/e = 17 ion current, i_{17}, in the mass spectrometer signal until no changes with time could be detected. After establishment of the pressure the sample was flashed to $\sim$1900°K, then allowed to cool to the predetermined temperature of the experiment. The interaction time was usually 5 - 10 minutes. Next, heating current to the crystal was terminated, LEED optics turned on and a photograph taken of the pattern on the fluorescent screen.

For interaction temperatures of $\sim$ 1100°K the crystal was observed to cool a maximum of 50° during the time between turning off the heating current and taking the photograph. At lower steady state temperatures this cooling was somewhat less. This procedure could lead to possible errors in correlating the LEED patterns with interaction temperatures, however in all experiments the patterns were not observed to change rapidly with such temperature differences and no errors are

believed to be due to this technique.

In experiments in which the total pressure was above $\sim 10^{-5}$ torr. electron bombardment could not be used to heat the sample. Instead, the light from a 1000 watt projector bulb was focused upon the backside of the crystal and was of sufficient intensity to heat the sample to $\sim 1000°$. Due to the placement of the projector bulb no photographs could be taken; only visual observations could be made.

RESULTS

Thermal Desorption of N_2 and H_2 from W(100)

The thermal desorption results of H_2 dosing of W(100) are shown in Fig. 4. During the adsorption interval the sample was somewhat hotter than 300°K, but the spectra are similar to those reported previously by Tamm and Schmidt (30) in which the sample was dosed at 300°K. In this system two desorption peaks occur at ~500°K and ~580°K and are identified as β_1-H and β_2-H respectively. No effort was made to calculate the number of adsorbed atoms in this case or any others since an accurate calibration of the mass spectrometer or ion gauge was not performed.

The desorption spectra due to the N_2 dosing of W(100) are shown in Figs. 5 and 6. Figure 5 shows results of the initial experiments on the N_2/W(100) system. For doses ≤5L. the spectra are representative of previously reported results. However, for larger doses it was uncertain why a second high temperature peak was present. Clavenna and Schmidt (41) reported that formation of this state, β_1-N, required a relatively large dose, ~2000L., of N_2. It was also known that hot filaments could excite the N_2 molecules and lead to creation of this state at lower doses. However, the precaution was always taken to make sure that all hot filaments were off during the adsorption interval.

Finally, it was discovered that ion pump operation was responsible for β_1-N being formed at such low doses. The spectra shown in Fig. 6 were obtained with the ion pump off during the adsorption interval, but turned on during the thermal flash for increased pumping speed. These spectra show the single high temperature peak at ~1200°K that is due to β_2-N desorption. The initial population of this state causes the desorption peak to shift to lower temperatures with increasing coverage which is a result of second order desorption kinetics. None of the spectra in Fig. 6 indicates that the surface is saturated with nitrogen, though for the highest dose it appears that a second peak may be present at ~980°K. This may be the result of the formation of some β_1-N that can be formed at very high doses (41).

Thermal Desorption of N_2 and H_2 from W(111)

The thermal desorption results of H_2 dosing of W(111) are shown in Fig. 7. The resolution of these curves into individual desorption peaks is incomplete due to the low pumping speed. However, it appears that peaks are present at 575°K and 515°K. A third peak may also be present at ~500°K. Previously reported results (34) using higher flash rates and pumping speeds showed a two peak spectrum, 350° and 500°K, for a surface dosed at 300°K. From these results it is believed that the W(111) sample in this system was free of any gross

contamination, though the comparison between the present and previously reported results is somewhat qualitative.

The thermal desorption of N_2 from W(111) is shown in Fig. 8. For very low doses, <1L., there is one high temperature peak at ~1300°K which shifts to lower temperatures with increasing coverage. Again, this is indicative of second order desorption kinetics and agrees with the results of Delchar and Ehrlich (39). With increasing doses a single peak occurs at ~1200° which shifts to higher temperatures with increasing coverages.

All of the spectra shown in Fig. 8 were obtained with the ion pump on during the adsorption interval. Since ion pump operation was shown to significantly effect N_2 adsorption on W(100), experiments were also performed in which the ion pump was off during the adsorption interval. In this case the only difference was that somewhat more nitrogen adsorbed if the ion pump was off. There were no differences comparable to those found in the N_2/W(100) system. The small peak at 900° in Fig. 8 may be the genesis of another nitrogen surface state, but if it is the result of ion pump operation it obviously requires a much greater dose for formation on (111) than on (100).

LEED Patterns from W(100) and W(111) Clean Surfaces

Figure 9a shows the LEED pattern from the clean W(100) surface at a primary beam energy of 46 eV. The specular beam is the lower of two intense spots near the center located at about 6:30. The upper of these two spots is the incandescent filament of the LEED electron gun. Figure 9b is a schematic representation of the LEED pattern in 9a and shows the indexing of the first order beams, some of which cannot be seen in 9a due to very low intensity. If the (100) plane were normal to the incident beam, a fourfold degeneracy of intensity would exist among the set $(1, 0)$ $(0, 1)$ $(0, \bar{1})$ $(\bar{1}, 0)$ and the set $(1, 1)$ $(\bar{1}, 1)$ $(1, \bar{1})$ $(\bar{1}, \bar{1})$. From inspection of the photo it is obvious that this degeneracy does not exist even for a (100) surface that is only a few degrees off normal incidence. Figure 9c is the unit cell chosen to index the diffraction pattern from (100).

The clean pattern from W(111) at 25 eV beam energy is shown in Fig. 10a. The specular beam is barely visible, but is located near the center of the pattern at about 6:30 below the intense spot due to the gun filament. Though not at normal incidence this pattern nearly displays the expected threefold intensity degeneracy among the beams of the set $(0, 1)$ $(1, 0)$ $(\bar{1}, \bar{1})$ and the set $(\bar{1}, 0)$ $(0, \bar{1})$ $(1, 1)$. Figures 10b and c show the indexing of the pattern and the surface unit cell.

LEED Patterns Resulting from the Interaction of H_2, N_2 and NH_3 with W(100)

The LEED patterns resulting when hydrogen adsorbs on W(100) are shown in Fig. 11. These patterns agree with previous results (29) in that initial adsorption leads to a C(2 x 2) pattern followed by splitting of the 1/2 order beams and finally a (1 x 1) due to a saturated surface. The occurrence of the C(2 x 2) has been reported as being very sensitive to surface contamination by CO (32). Trace amounts of only a few percent will preclude the C(2 x 2)-H formation. This fact along with the TDS results for H_2 on W(100) is very good evidence that the (100) surface used in this system was quite clean.

The adsorption of N_2 on W(100) at temperatures $\leq 600°K$ resulted in the expected C(2 x 2) pattern (40). However, there was a correlation between the LEED and TDS results with respect to ion pump operation during the adsorption interval. If the ion pump was on a C(2 x 2) is observed for low doses <10L., but for doses >50L. a (1 x 1) pattern results. This (1 x 1) structure corresponds to the same surface state that gives two high temperature desorption peaks.

The LEED patterns which are observed when N_2 interacts with W(100) in a steady state manner are shown in Fig. 12. P_{N_2} was $\sim 10^{-6}$ torr. for all patterns shown. Above 1000°K the C(2 x 2) pattern is all that is observed. Below 1000°K the 1/2 order beams are still present,

but additional fractional order spots are present, also. It appears that this pattern is still barely detectable at 700°K where all spots have considerably less intensity. During the experiments the ion pump and all hot filaments were off except for the thermionic emitter used to heat the sample.

When ammonia interacts with W(100) at steady state pressures 10^{-6} - 10^{-3} torr. and temperatures 700° - 1200°K a number of surface structures are formed. Above 1100°K and pressures $\leq 10^{-5}$ torr. a C(2 x 2) pattern is observed initially as the crystal cools. For temperatures of 1000° - 1100°K and 10^{-6} torr. ammonia pressure a 1/6 order pattern is present initially. Figure 13 shows the complete sequence of patterns observed at this pressure and temperatures 700° - 1100°K. It is observed that as the temperature is decreased the fractional order beams tend to move in such a way as to create nearly a 1/5 order pattern. For $P_{NH_3} \gtrsim 10^{-4}$ torr. and temperatures $\leq$ 1000°K a (3 x 1) pattern is usually observed. This pattern is sometimes very streaked and fades rapidly (~20 sec.) as the crystal cools in the ammonia ambient. At the highest ammonia pressures of $\sim 10^{-3}$ torr. a weak (1 x 1) is present initially or no diffraction beams are present. Thus, the surface structure must be highly disordered at these pressures.

The presence of a 1/6 order pattern in the NH_3/W(100) system

was observed previously by Estrup and Anderson (4). Their experimental procedure was somewhat different from the one used in this investigation. In their system the W(100) was dosed at 300°K with ammonia pressure $\sim 10^{-8}$ torr. The sample was then heated to ~1000°K and a 1/6 order pattern resulted.

LEED Patterns Resulting from the Interaction of H_2, N_2 and NH_3 with W(111)

Whenever H_2 or N_2 are allowed to adsorb on W(111) at temperatures $\leq 600°K$ no new diffraction beams occur. These experiments were performed with respective partial pressures $10^{-9} - 10^{-5}$ torr. and pattern observation was made at various primary beam energies from 10 eV to 100 eV. Thus, even though the TDS results indicated that chemisorption of H_2 or N_2 had occurred the LEED results indicated that the surface structures were either disordered or simple (1 x 1) arrays.

The next step was to see if ordered structures might be formed if N_2 were allowed to interact in a steady state manner with W(111) at $P_{N_2} = 10^{-6} - 10^{-5}$ torr. and temperatures 700° - 1300°K. At 10^{-6} torr. no ordered patterns were detected over the entire temperature range. However, at 10^{-5} torr. a well ordered (3 x 3) pattern is formed if the crystal is maintained at ~1300°K during the interaction interval. Figure 14 shows all the patterns formed at 10^{-5} torr. for every 100°

interval from 700° - 1300°K. It is observed from these photos that an ordered state begins to develop at 1000°K with some well-developed spots and a considerable background intensity. At 1200° several elongated spots are present at the 1/3 order positions. This structure is transitional between the one at 1000° and the (3 x 3) at 1300°K since some of the spots in the 1000°K pattern are not located at the 1/3 order positions. It is interesting to note that the (3 x 3) pattern can only be observed when the crystal has cooled to ~900°K after interaction at 1300°. This contrasts with the results on the (100) surface in which ordered patterns are observed while the crystal is still considerably above 900°. Either the Debye-Waller temperature factor is significantly greater for structures on the (111) than on the (100) or the surface atoms in this (3 x 3) structure do not become ordered above ~ 900°K.

Examination of the well developed (3 x 3) pattern shows that the rotational symmetry is still threefold judging from systematic intensity variations that are present even though the surface is not normally oriented toward the primary beam. The photo also shows that a considerable amount of energy has been extracted from the specular beam since the (0, 0) spot is not detectable.

These experiments with nitrogen were also performed with the ion pump on during interaction. There were no significant differences

in the LEED patterns.

Two well ordered structures are formed when ammonia interacts with W(111) at pressures 10^{-6} - 10^{-3} torr and temperatures 700° - 1400°K. At ~1350°K the same (3x3) structure can be formed by ammonia as was observed in the N_2/W(111) system. However, ammonia can also form an additional ordered state at ~1000°K. Its LEED pattern is shown in Fig. 15a. For comparison Fig. 15b shows the partial indexing of the substrate and superstructure spots. This structure occurs over a considerable pressure range, 10^{-6} - 10^{-3} torr. Its maximum intensity shifts ~100° toward higher temperatures with increasing ammonia pressures. When formed at 10^{-3} torr. it fades in ~30 sec. if the crystal cools in the 10^{-3} torr. ammonia ambient. Its presence can be greatly increased by lowering the ammonia pressure to $\lesssim 10^{-5}$ torr. in a very short time after heating is terminated. In this case the pattern has been observed for times up to 5 minutes. Even after fading at these lower pressures it can be regenerated by heating the crystal to ~900°K. Presumably, this treatment only removes weakly adsorbed species from "on top" of the ordered structure. It is apparent that NH_3 or N_2 have very low sticking coefficients, $\sim 10^{-4}$, on this structure.

DISCUSSION OF RESULTS

The previous section has shown that structural changes can be detected by the LEED technique when ammonia or nitrogen interacts with W(100) and (111) single crystal surfaces. It is the purpose of this section to consider what are the atomic arrangements in these surface structures. The qualitative nature of LEED does not allow for an unambiguous assignment of structures from these diffraction results and it must always be borne in mind that in general several structural types could satisfy individual diffraction results. However, this discussion will in most cases only consider one model for each particular interaction. The first part will consist of comments on the general approach and assumptions used in determining the surface structures. This will be followed by an explicit discussion of the diffraction results for each interaction. The last part will be a summary and comparison between the results and interpretations of this investigation and those obtained previously by others on the same ammonia-tungsten interaction system.

General Approach to the Interpretation of the LEED Patterns

Interpretation of the results of this investigation will involve a number of assumptions. First of these will be the supposition that the tungsten atoms of the surface layer and topmost sublayers are responsible for scattering nearly all the electrons that constitute the

diffraction patterns. This assumption is somewhat arbitrary, but in the absence of positive proof that multiple scattering is significant it is considered to be reasonable. Also, multiple scattering will be ignored completely since diffraction from all structural models can be explained in terms of simple kinematical considerations.

Nearly all interpretations will be in terms of models that involve the placement of a simple uniform overlayer structure upon a known substrate geometry. In previous LEED literature this has been termed the "coincident lattice" model (50). The basic assumption is that the atoms in the surface layer interact with one another in such a manner as to form an overlayer structure that in general ignores the two dimensional periodicity of the substrate. Thus, atoms in the surface overlayer may not always reside on substrate sites of high symmetry that tend to maximize the bonding coordination of the surface to substrate atoms. In such models there is only an occasional coincidence between lattice points of the surface and substrate structures respectively. There will be an increase in the interfacial energy of such systems as compared to those which have the surface atoms at symmetric sites of the substrate. In order that the total energy of the system be minimized it is argued that rearrangement of the original surface atoms due to adsorbate bonding results in a decrease of energy in excess of that created by the interfacial strain.

Generally the area density of tungsten surface atoms in the rearranged surface structure will not be equal to that of the clean unrearranged surface from which it was formed. If the new structure has a higher density, then it is assumed that the new lattice is not perfect, but has defects resulting from the vacancy of atoms from some surface sites. These defects have the highest probability of occurrence at sites which allow a minimum of coordination between the surface and substrate atoms. It is also likely that such sites result in a significant protrusion of the surface atom above surrounding surface atoms creating enhanced strain in the surface layer and a further increase in the system energy. All surface structures to be proposed have a higher local surface density and it will be assumed that defects due to vacancies will account for there being no net change in the average density. In their study of bulk nitride systems Khitrova and Pinsker (51) found that defect structures were quite common. All illustrations in the dissertation will show the perfect fully occupied surface structures and only obvious defect sites will be identified if possible.

As a prelude to discussing the diffraction results a simple idealized example will be given to show how the diffraction from two periodic structures (surface + substrate) may result in an apparently complex diffraction pattern that contains many diffracted beams not representative of either structure independently, but result from the

interaction of the incident radiation with the total system. Only single scattering events will be considered allowing the use of equations of kinematical theory to permit the directions of the diffracted beams to be calculated. The angular and wavelength dependencies of the atomic scattering factors will be ignored since all that is being sought are the positions of the beams in the diffraction pattern. Only the phase factors are considered. The model is one dimensional, but can easily be generalized to two dimensions.

The substrate is taken to be a linear chain of point scatterers separated by the periodic distance a. Upon this substrate is placed the surface linear array with unit spacing a'. The superperiod coincidence is given by the relationship, $ma = na'$. Thus, every m substrate periods coincide with n surface periods. The first step is to calculate the diffracted amplitude from each lattice ignoring the spacing between the lattices which has no effect on diffraction angles. Let f' and f be the amplitude from the surface and substrate respectively:

$$f'(h) = \sum_{p}^{N'} \exp 2\pi i h a' p \qquad (13a)$$

$$f(h) = \sum_{q}^{N} \exp 2\pi i h a q \qquad (13b)$$

where h is the parameter in diffraction space denoting beam positions. Its complete definition as used here is given by $h = (s-s_o)/\lambda$. N', N

are the number of scatterers in the surface and substrate arrays respectively. The total amplitude is the sum of the two parts above times a phase factor representing the superperiod:

$$F(h) = \left(\sum_{p}^{N'=n} \exp 2\pi i h a' p + \sum_{q}^{N=m} \exp 2\pi i h a q \right) \sum_{r}^{M} \exp 2\pi i h m a r \ .$$

In simple terms this is nothing more than the sum of amplitude from M unit cells each of periodicity ma (na') which contains n surface points and m substrate points. The complex square, $F(h)*F(h)$, gives the diffracted intensity, I(h), discounting the effect of the ignored atomic factors and spacing between arrays:

$$I(h) = \left(\frac{\sin^2 \pi h a' n}{\sin^2 \pi h a'} + \frac{\sin^2 \pi h a' m}{\sin^2 \pi h a'} + \frac{\sin \pi h a' n \sin \pi h a m}{\sin \pi h a' \sin \pi h a} \right) \qquad (14)$$

$$\times \frac{\sin^2 \pi h m a M}{\sin^2 \pi h m a} \ .$$

From the form of I(h) it is observed that the total system will result in diffraction maxima at positions proportional to integral multiples of: 1/a, 1/a' and 1/ma. The first two positions result from the independent diffraction of the substrate and surface respectively. The last positions, α1/ma, may or may not be observed even in this simple example depending upon the distributed widths of the interference functions from each lattice which are proportional to 1/n or 1/m for each function respectively. Thus, if n and m are small compared to M the superperiod beams will be centered very near positions α 1/ma

and are known as fractional order beams. A refined calculation in which many of the presently neglected factors are included would be needed when considering a specific diffraction system, however this discussion has shown how a pattern containing many fractional order beams may be due to the combination of two simple systems.

Structures Resulting from the Interaction of Ammonia with W(100)

Figure 13e is an apparent complex pattern which displays nearly (6x6) periodicity and may be the result of diffraction from a surface structure whose unit cell periodicity was (6x6) and area that was 36 times that of the (100) substrate cell area. Obviously, this would result in the possibility of all the fractional order beams occurring in the pattern. However, the previous discussion has shown that diffraction from a superstructure consisting of simple surface and substrate geometries may also be used to explain such patterns. Intuitively, it also seems more probable that surface interactions are significant only over a few atomic diameters as compared to say a true (6x6) surface periodicity that implies very long range interactions. Therefore, the simple overlayer approach will be pursued.

Figure 16a shows one unit cell of a superstructure that has exact (6x6) periodicity. The fourfold (100) substrate is indicated by the solid lines with the intersections of lines representing the centers of substrate

tungsten atoms. 36 unit cells of the substrate are contained in the superstructure unit and since the total periodicity is (6x6), beams should occur in the diffraction pattern at every (1/6, 1/6) position with respect to substrate beam indexing. This is very close to the beam positions occurring in 13d and e. The surface structure unit cell is nearly hexagonal with an angle of 64° between close packed rows as compared to the undistorted hexagonal value of 60°.

Hexagonal overlayer structures on fourfold substrates have been proposed previously for other surface systems (18, 52). The mechanism of their formation is not well understood and neither are the energetics of overlayer to substrate bonding. Their proposed existence is usually based upon the fact that hexagonal forms with similar bond distances are found in chemically related bulk systems or the assumed idea that such a close packed surface layer will result in a reduction of system energy. Khitrova and Pinsker (51) have discovered that a number of bulk nitride structures may be formed if ammonia or nitrogen reacts with tungsten films at high temperatures, T ~1100°K, and atmospheric pressures. These phases, δ, were all characterized by layers of hexagonal packed tungsten atoms. The intralayer W-W bond distance in all structures was ~2.9Å. The close packed spacing in bcc tungsten is 2.74Å. The model of 16a results in a W-W bond of 2.98Å.

There are 45 surface tungsten atoms in the superstructure unit

of 16a. Since there were only 36 in this same area on the clean surface, there must exist 9 vacant sites if average surface atom density is to be conserved. It is not obvious where all nine vacancies exist and the defect distribution is probably somewhat random. There are what appear to be obvious sites of relatively poor bonding character and these are indicated. Surface tungsten atom bonding at these sites would result in low coordination to the substrate and a protrusion of the surface atom above surrounding neighbors to further decrease the bonding capability of these sites.

The patterns of Figs. 13a - c show that as the temperature of interaction is lowered the system periodicity approaches fifth order and the pattern is ill defined at 700°K except possibly for reflections close to the substrate spots. The pattern almost appears to be (5 x 1), but is not exactly because the spacing between all the fractional order beams is not equal nor are they located at the 1/5 order positions. There are also very weak reflections not located along the (h0) or (0k) axes. These non-axial beams are not due to a small number of sixth order domains remaining on the surface since the beam positions do not coincide with those in the sixth order pattern. However, for the purposes of this discussion the patterns 13a - c will be assumed to be due to a fifth order surface structure.

It is possible that these lower temperature patterns are due to

a slight contraction of the hexagonal surface of 16a to form a superstructure of nearly (5 x 5) periodicity. Such an overlayer structure would now have a W-W bond distance of 2.76Å. This would be very nearly the close packed spacing in pure tungsten, but the defect vacancies would be expected to allow for an increase in this value.

Figure 16b shows another structure that qualitatively agrees with the assumed fifth order periodicity. In this case the superstructure unit cell is a (5 x 1) since there are five substrate spacings along one direction and only one along the other. Diffraction beams from this superstructure would have 1/5 order periodicity only along one axis of the diffraction pattern. The beam spacing along the other axis would equal that of the substrate spacing since all lattice points of the substrate and surface are coincident along the direction normal to the fifth order periodicity. The diffraction pattern will still display fourfold symmetry and have 1/5 order beams along both axes due to the fact that other (5 x 1) regions will exist on the fourfold substrate rotated 90° with respect to the one shown in 16b. Energetically, there is no difference between the two placements and they are both equally probable.

The exact coincidence of five substrate units and six surface units would lead to a W-W bond length of 2.63Å along this direction in the surface structure. This distance is too small and it must be argued that either the surface defective positions relieve this strain or the

surface atoms do not all lie in a straight line in this direction. With atoms in a straight line the removal of one atom per (5 x 1) unit cell would appear to create such a gap that the remaining atoms would prefer to redistribute themselves to their original clean surface positions resulting in a (1 x 1) structure. However, if the atoms did not line up exactly, but instead formed some type of zig-zag pattern along this direction an increased W-W bond length would be allowed. It is this argument which has lead to the proposal of a (5 x 5) hexagonal structure similar to 16a to account for the diffraction results of 13a - c, since a zig-zag displacement along the fifth order direction tends to make the surface structure approach the hexagonal form.

Heretofore, all discussion has been concerned with the placement of the surface tungsten atoms since it was originally assumed that the heavy metal atoms were responsible for nearly all the diffracted intensities. An equally relevant matter now to be considered is the location of the bonding sites of surface nitrogen that result in rearrangement of the tungsten surface.

For the surface structures being considered here there is very little previous information to guide one in determining the nitrogen bonding sites. A recent semiempirical quantum mechanical calculation showed that a single nitrogen atom on a finite tungsten square array prefers to bond in the "fourfold hole" on the (100) surface (53). This

site is the slightly distorted octahedral position at the face of the cubic bcc unit cell; as a surface site on W(100) it has a square array of four tungsten atoms in the surface plane and a single atom centered below at ~1.58Å. Nitrogen occupation of every other one of the sites correlates well with the C(2x2) structure formed by nitrogen adsorption at ~300°K on W(100). Khitrova and Pinsker (51) found that in the bulk tungsten nitrides nitrogen generally prefers trigonal or sixfold coordination to tungstens. The trigonal bonding is the result of nitrogen placement at the apex of a trigonal pyramid whose base is formed by three tungstens. Sixfold coordination results when nitrogen is placed at the center of a trigonal based prism, the ends of which consist of three tungsten atoms each.

For the hexagonal structure of Fig. 16a it is quite probable that nitrogen atoms would prefer to bond above the centers of trigonal arrays of surface tungsten atoms. These sites would appear to maximize the coordination of the nitrogen-tungsten bonding compared to other available positions. The most favorable bonding array probably does not result in nitrogen atoms at every trigonal site. In the case of nitrogen bonding on W(100) at 300°K the atoms occupy only half the fourfold sites. Also, bonding at every trigonal array would create a stoichiometry of WN_2 and at present there is no evidence from other investigations of such a high surface nitrogen content. Three nitrogens

per hexagonal unit cell result in WN stoichiometry and this is believed to be a more realistic value. It would be assumed that the three nitrogens are arranged in a threefold manner within each cell. A later discussion concerned with the relationship between surface structures and ammonia decomposition mechanism will again consider this matter of nitrogen bonding.

Structures Resulting from the Interaction of Nitrogen and Ammonia with W(111)

Patterns in Fig. 14 show that the interaction of nitrogen with W(111) below T ~900° K does not result in any new diffraction beams observed. Instead, adsorption has caused three of the beams of the clean pattern, (11), $(\bar{1}0)$ and $(0\bar{1})$, to become extinguished. Thus, a (1 x 1) pattern exists with its threefold symmetry more pronounced than in the clean patterns. This is probably the result of nitrogen atom bonding in every other trigonal site. Figure 17a shows one possibility for this bonding scheme. The nitrogen bonding on this surface is assumed to be similar to nitrogen-tungsten interaction on W(100) in that the nitrogen atom appears to prefer sites of maximum coordination to tungsten atoms. The trigonal bonding sites chosen in 17a present the possibility of nitrogen coordination to four tungsten atoms: three in the plane with equilateral spacing of 4.47Å and one centered below the plane at ~1.82Å.

The remaining trigonal sites are identical except the subsurface atom is ~3.64Å below the surface and this increased interaction distance would not appear to be as capable of bonding the nitrogens as the sites that have been chosen.

The patterns of Figs. 14d - g show that as the temperature of nitrogen interaction is increased at $P_{N_2} \sim 10^{-5}$ torr. a well-defined (3 x 3) pattern finally develops at ~ 1300° K. Ammonia interaction at this temperature and pressure is also capable of forming the same structure. This structure may be the result of a partial coverage of the high bonding energy state of Fig. 17a since Fig. 8 shows that 1150° - 1300° K is the temperature range of desorption of this state. A simple explanation would attribute the (3 x 3) pattern to a removal of eight-ninths of the nitrogen atoms in 17a leaving the one ninth remaining atoms at identical sites separated by three lattice spacings. Such an adsorbate pattern would result in a spacing of 13.5Å between the nitrogen atoms and it is not obvious how such a large spacing could result in a periodic structure though spacings of this order have apparently been found on other tungsten nitride surface systems (44).

Alternatively, the (3 x 3) structure could be the result of a rearranged surface. One possible choice that does not involve a total rearrangement is shown in Fig. 17b. The dashed lines show one (3 x 3) unit cell which in this case is the periodicity of the surface or

superstructure unit cell. 17c shows the clean surface structure and arrows to indicate the movement of certain atoms in forming the (3 x 3) structure. The open circles of 17b represent original subsurface tungsten atoms that now have considerably more exposure in the (3 x 3) structure. There is no reason not to expect these exposed atoms to participate in nitrogen bonding and it may even be the case that certain of them are displaced toward the surface from their original positions due to adsorbate interactions.

Figure 15a shows that ammonia interaction at ~1000°K is capable of forming a well ordered structure that is absent in the molecular nitrogen-W(111) interaction system. The diffraction pattern has hexagonal symmetry which is rotated 30° with respect to that of the substrate. The partial indexing of this pattern is shown in 15b and it can be seen that there is an intense array of hexagonal spots at positions of 4/5 that of the substrate second order spots. Due to their high intensity it would seem reasonable to conclude that these beams are due to first order diffraction from a hexagonal overlayer structure that is rotated 30°. If that is the case then a calculation of the surface structure lattice parameter from the diffraction pattern gives a value of 2.83Å. Diffraction patterns at other beam energies show that the spacing between (0, 0) and the first order substrate beams is divided into five spacings as the result of the surface structure presence on the

substrate. Thus, the superstructure periodicity would be (5 x 5). Figure 18 is a possible structure that may result in the fifth order periodicity. This is one unit cell of the (5 x 5) superstructure where the substrate is represented by the straight lines. As an aid in visualizing the rotated surface structure a triply primitive unit cell of the surface has been indicated which has sides colinear with the substrate unit cell directions. Obviously, this is not the smallest repeat unit of the surface structure, but it has the advantage in that the rotation of the surface structure has been eliminated. The smallest repeat distance of this surface structure is ~3.2Å and is close enough to 2.83Å to be within the experimental accuracy of this LEED system which is generally thought to involve an uncertainty of ~ 10% in such measurements. The (5 x 5) periodicity of the superstructure should result in fractional order beams at every (1/5, 1/5) positions. However, a sequence of patterns observed over a 20 - 30 eV beam energy range show that nearly all the 1/5 order beams are present only in small energy ranges of 5 - 10 eV. The pattern of 15a will not necessarily have the same fractional order beams as one obtained at a somewhat different energy, but was chosen to illustrate the hexagonal symmetry of the overlayer and the intense beams believed to be due to the nearly first order diffraction from the overlayer structure.

The matter of nitrogen bonding on the rearranged W(111) surface

structures will not be considered in detail, since it is believed that bonding on these hexagonal overlayers is probably very similar to that on the hexagonal overlayers proposed for the W(100) surface. A reasonable justification for this assumption will be given in a discussion concerned with the relationship between the surface overlayers and the kinetics of ammonia decomposition on W(100) and (111).

The Relationship Between the Proposed Structures and Results of Previous Investigations

Although the qualitative nature of the LEED technique prevents the exact determination of surface structures there are some results of this investigation that are independent of interpretation and have some relationship to previous investigations of the ammonia-tungsten interaction.

First, it was previously implied that ammonia decomposition on W(100) at pressures $\gtrsim 10^{-6}$ torr and $T \sim 700° - 1000°$ took place on a (1 x 1) surface structure (1). The results shown in Fig. 13 indicate this is clearly not the case. This is only an apparent contradiction, because the previous conclusion was not deduced from experiments involving steady state interaction. Also, at $T \sim 1000°K$ and $P_{NH_3} \simeq 10^{-4}$ torr. there is apparently a structural transformation on W(100) from the fifth order structures observed at lower pressures. "Apparently" is used here because experiments in this system at these pressures did not give

reproducible results. In the results section it was noted that a (3 x 1) or disordered structure was observed. However, there was never any high degree of reproducibility on (100) with respect to these higher pressure observations and for that reason no structures were proposed. This may be a problem of contamination, especially CO adsorption, since some degree of nonreproducibility was also present at lower pressures, but was generally not bothersome if CO background was relatively low, $\lesssim 10^{-9}$ torr. If the structural transformation is due to only the ammonia-tungsten interaction then it is reasonable to expect that the rate or even the mechanism of ammonia decomposition would also undergo a change at similar reaction conditions. At present, there are no kinetic results on W(100) at these pressures to check this postulate.

Second, the surface structure occurring on (111) at ~1000°K did not undergo any transformations as the ammonia pressure was increased from 10^{-6} to 10^{-3} torr. Thus, it would be expected that at least the mechanism of decomposition on W(111) would remain the same over this pressure range although the rate may vary due to a changing surface concentration of the active species forming the transition state. McAllister and Hansen (3) claimed to have found a zero order dependence of rate upon ammonia pressure in this range. This correlates well with the idea that the surface is saturated with the active species and that the (5 x 5) structure on (111) occupied nearly all the surface.

A relationship between the hexagonal structures proposed in this investigation and previous kinetic results will now be considered. The results of Peng and Dawson (47) on a polycrystalline wire indicated that a surface of W_2N_3H could be produced by very heavy doses, $\sim 10^6$ L, of ammonia at $\sim 700°$K. Kinetic rate measurements on W(100), (110) and (111) by McAllister and Hansen (3) were explained by postulating that the rate determining step of ammonia decomposition on all faces was:

$$W_2N_3H_2 \rightarrow W_2N + N_2 + H_2$$

where: $P_{NH_3} \simeq 10^{-3} - 10^{-1}$ torr. and $T \simeq 800° - 1000°$K. At somewhat lower pressures the second order decomposition of WN was predominant:

$$2WN \rightarrow W_2N + \tfrac{1}{2}N_2 .$$

Figure 19 shows a single unit cell of a hexagonal tungsten surface array. With three nitrogens bonded at symmetrically disposed trigonal sites the stoichiometry of the unit is WN since there are only three tungsten atoms per hexagonal cell. Molecular desorption from this structure could result from the migration of one nitrogen to an adjacent site which would then also be adjacent to another adsorbed nitrogen. Nitrogen-nitrogen bonds could then form and molecular desorption would occur. For most of the hexagonal structures proposed in this dissertation the nitrogen separation on adjacent sites would be ~ 1.5Å. This would seem to be a favorable distance for the transition state.

A state of nearly W_2N_3 stoichiometry could be produced by the addition of one nitrogen atom to the hexagonal cell. If only the five local tungsten atoms are considered to participate in the transition state then the stoichiometry created by the additional nitrogen would be $W_{7/3}N_3$; desorption of N_2 would leave $W_{7/3}N$. Tungsten-to-nitrogen ratios for these structures are 17% higher than for the W_2N_3 and W_2N reported, but are doubtless within experimental errors for the reported structures.

The location of surface hydrogen on these hexagonal arrays is a somewhat more difficult matter to consider. This is mainly due to the fact that atomic hydrogen possesses considerable mobility on tungsten at the temperatures of this investigation. For states other than $W_2N_3H_2$ hydrogen is probably randomly distributed on the surface with second order collisions and molecular desorption occurring at a large number of different sites. For $W_2N_3H_2$ it may be the case that the two hydrogens are bonded to the incoming nitrogen atom shown in Fig. 19. Their presence on the nitrogen would occur as the result of incomplete dehydrogenation of the ammonia molecule upon initial surface interaction.

FUTURE INVESTIGATIONS

The results of this investigation have shown that a number of different surface structures may be formed on W(100) or W(111) due to ammonia or nitrogen interaction. Though surface structures were proposed to qualitatively account for the diffraction data, there are some aspects of the interpretations given here which could form a basis for future investigations of this system.

One of the more general approaches for future work could involve an effort to extend the present knowledge of LEED in order that more quantitative structural information could be obtained from the diffraction data. There have been a number of serious attempts in this direction during the last decade but progress to date has been unimpressive and prospects for major successes in the near future therefore do not seem bright. Alternatively, it would be a significant accomplishment if one were able to develop a technique for identifying whether reconstructed surface layers were present without actually determining the structure. This has been an area of very little concern by those involved with advancing the quantitative understanding of the LEED process. Since reconstructed surface layers have been proposed for a number of surface systems, the development of such a technique would have general applicability.

Another area of future investigation could be directed toward

calculations of surface energies and the mechanisms of forming reconstructed surfaces. Interpretations of the present results were obtained without quantitative information concerning the energetics of surface structures. Again, investigations in this direction would probably have general application to a number of surface catalytic systems.

Results of this investigation have shown that adsorbed contaminants may influence the surface structures in the ammonia-tungsten system. Specifically, the interaction of ammonia with W(100) at pressures $> 10^{-5}$ torr. indicate that coadsorption of CO may lead to unreproducible results. Whether this is actually the case could be determined by using the technique of Auger electron spectroscopy (AES). This technique can chemically identify all surface species except hydrogen or helium at surface concentrations of 1% or less. The results on W(111) were quite reproducible compared to those on W(100) and this may be the result of a higher specificity of a given contaminant for the W(100) surface. It would be a simple matter to confirm this possibility using AES.

BIBLIOGRAPHY

1. K. Matsushita and R. S. Hansen, J. Chem. Phys., 52, 4877 (1970).

2. P. T. Dawson and R. S. Hansen, J. Chem. Phys., 48, 623 (1968).

3. J. McAllister and R. S. Hansen, J. Chem. Phys., 59, 414 (1973).

4. P. J. Estrup and J. Anderson, J. Chem. Phys., 49, 523 (1968).

5. J. W. May, R. J. Szostak and L. H. Germer, Sur. Sci., 15, 37 (1969).

6. C. Kittel, Introduction to Solid State Physics, 3rd ed. (John Wiley and Sons, Inc., New York, N. Y., 1968).

7. G. A. Somorjai and H. H. Farrell, Advan. in Chem. Phys., 20, 215 (1971).

8. P. J. Estrup and E. G. McRae, Sur. Sci., 25, 1 (1971).

9. J. W. May, Advan. in Catalysis, 21, 152 (1970).

10. K. Hirabayashi and Y. Takeishi, Sur. Sci., 4, 150 (1966).

11. E. G. McRae, J. Chem. Phys., 45, 3258 (1966).

12. M. Lax, Rev. Mod. Phys., 23, 287 (1951).

13. G. A. Somorjai and F. J. Szalkowski, J. Chem. Phys., 54, 389 (1971).

14. E. A. Wood, J. Appl. Phys., 35, 1306 (1964).

15. J. J. Lander, Progress in Solid State Chem., 2, 26 (1965).

16. R. L. Park and H. H. Madden, Sur. Sci., 11, 188 (1968).

17. L. H. Germer, J. W. May and R. J. Szostak, Sur. Sci., 8, 430 (1967).

18. A. E. Morgan and G. A. Somorjai, Sur. Sci., 12, 405 (1968).

19. R. L. Park, J. Appl. Phys., 37, 295 (1966).

20. R. L. Park and H. E. Farnsworth, Sur. Sci., 2, 527 (1964).

21. J. E. Houston and R. L. Park, Sur. Sci., 26, 269 (1971).

22. J. E. Houston, G. E. Laramore and R. L. Park, Sur. Sci., 34, 477 (1973).

23. J. Anderson and W. E. Danforth, J. Franklin Inst., 279, 160 (1965).

24. W. G. Frankenburg, in Catalysis, edited by P. H. Emmet (Reinhold Publ. Corp., New York, N. Y., 1955) Ch. 6, Vol. 3.

25. C. Bokhoven, C. van Heuden, R. Westrik and P. Zwietering, in Catalysis, edited by P. H. Emmet (Reinhold Publ. Corp., New York, N. Y., 1955) Ch. 7, Vol. 3.

26. A Mittasch, Adv. in. Catalysis, 2, 82 (1950).

27. A Nielsen, Adv. in. Catalysis, 5, 1 (1955).

28. G. C. Bond, Catalysis by Metals, (Academic Press, New York, N. Y., 1962) Ch. 16.

29. P. J. Estrup and J. Anderson, J. Chem. Phys., 45, 2254 (1966).

30. P. W. Tamm and L. D. Schmidt, J. Chem. Phys., 51, 5353 (1969).

31. D. L. Adams and L. H. Germer, Sur. Sci., 23, 419 (1970).

32. K. Yonehara and L. D. Schmidt, Sur. Sci., 25, 238 (1971).

33. T. E. Madey, Sur. Sci., 36, 281 (1973).

34. P. W. Tamm and L. D. Schmidt, J. Chem. Phys., 55, 4253 (1971).

35. R. M. Stern, J. Vac. Sci. & Tech., 2, 286 (1965).

36. K. J. Matysik, Sur. Sci., 29, 324 (1972).

37. D. L. Adams, J. W. May and L. H. Germer, Sur. Sci., 22, 45 (1970).

38. R. R. Rye and B. Barford, Sur. Sci., 27, 667 (1971).

39. T. A. Delchar and G. Ehrlich, J. Chem. Phys., 42, 2686 (1964).

40. P. J. Estrup and J. Anderson, J. Chem. Phys., 46, 567 (1967).

41. L. R. Clavenna and L. D. Schmidt, Sur. Sci., 22, 365 (1970).

42. P. W. Tamm and L. D. Schmidt, Sur. Sci., 26, 286 (1971).

43. D. A. King and M. G. Wells, Sur. Sci., 29, 454 (1972).

44. D. L. Adams and L. H. Germer, Sur. Sci., 27, 21 (1971).

45. J. C. Jungers and H. S. Taylor, J. Am. Chem. Soc., 57, 679 (1935).

46. R. M. Barrer, Trans. Faraday Soc., 32, 490 (1936).

47. Y. K. Peng and P. T. Dawson, J. Chem. Phys., 54, 950 (1971).

48. C. C. Chang, Ph. D. Thesis, Cornell University (1967).

49. K. Matsushita and R. S. Hansen, J. Chem. Phys., 52, 3619 (1970).

50. C. W. Tucker, J. Appl. Phys., 37, 528 (1966).

51. V. I. Khitrova and Z. G. Pinsker, Soviet Phys. Crystallography, 4, 513 (1959).

52. M. Boudart and O. F. Ollis, in The Structure and Chemistry of Solid Surfaces, edited by G. Somorjai (John Wiley and Sons, Inc., New York, N. Y., 1969).

53. L. Anders, Ph. D. Thesis, Iowa State University (1973).

APPENDIX: FIGURES

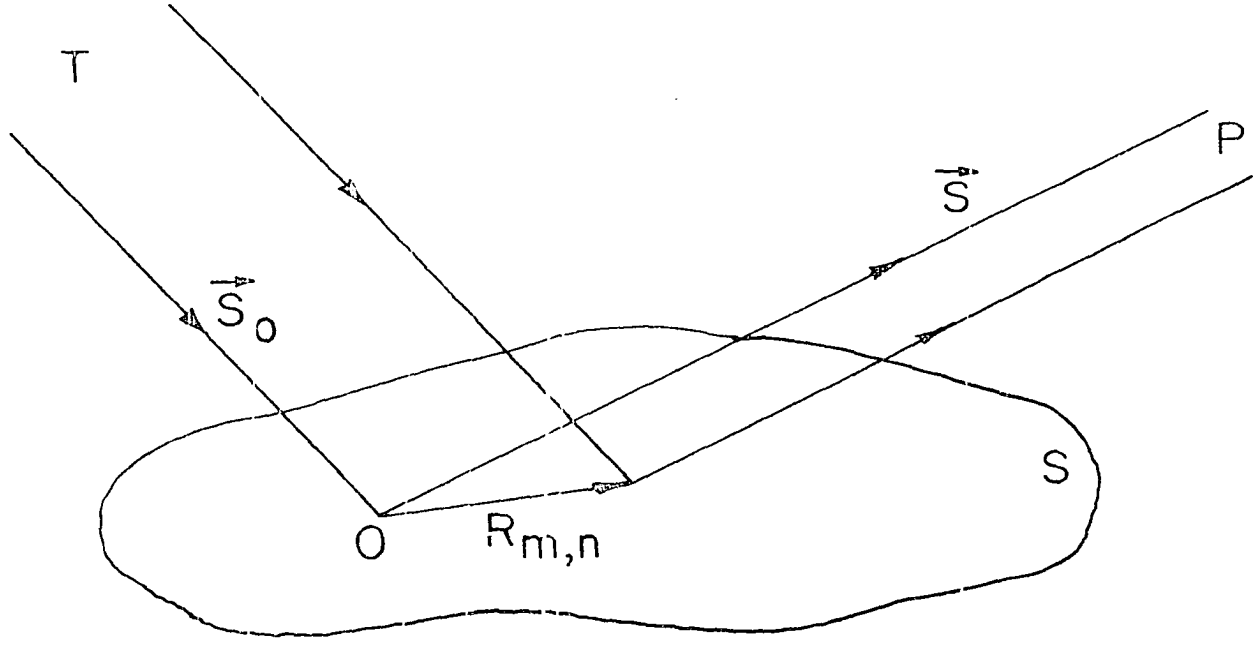

Fig. 1. Planar section, S, of two dimensional lattice. Incident and diffracted wavevectors are $\vec{s}_o$ and $\vec{s}$ respectively. $\vec{R}_{m,n}$ is a surface vector that denotes the displacement of atom (m, n) from origin, O.

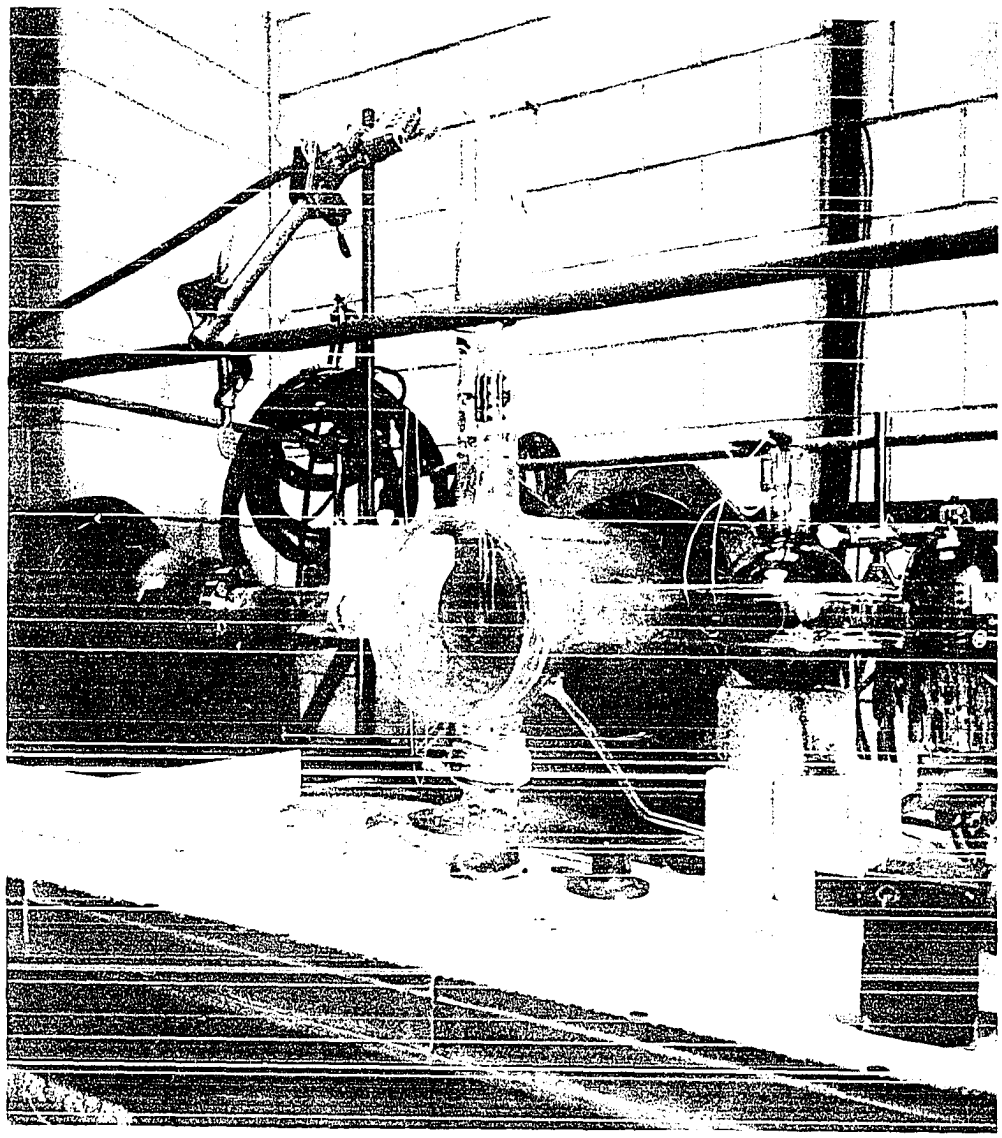

Fig. 2. Experimental LEED system.

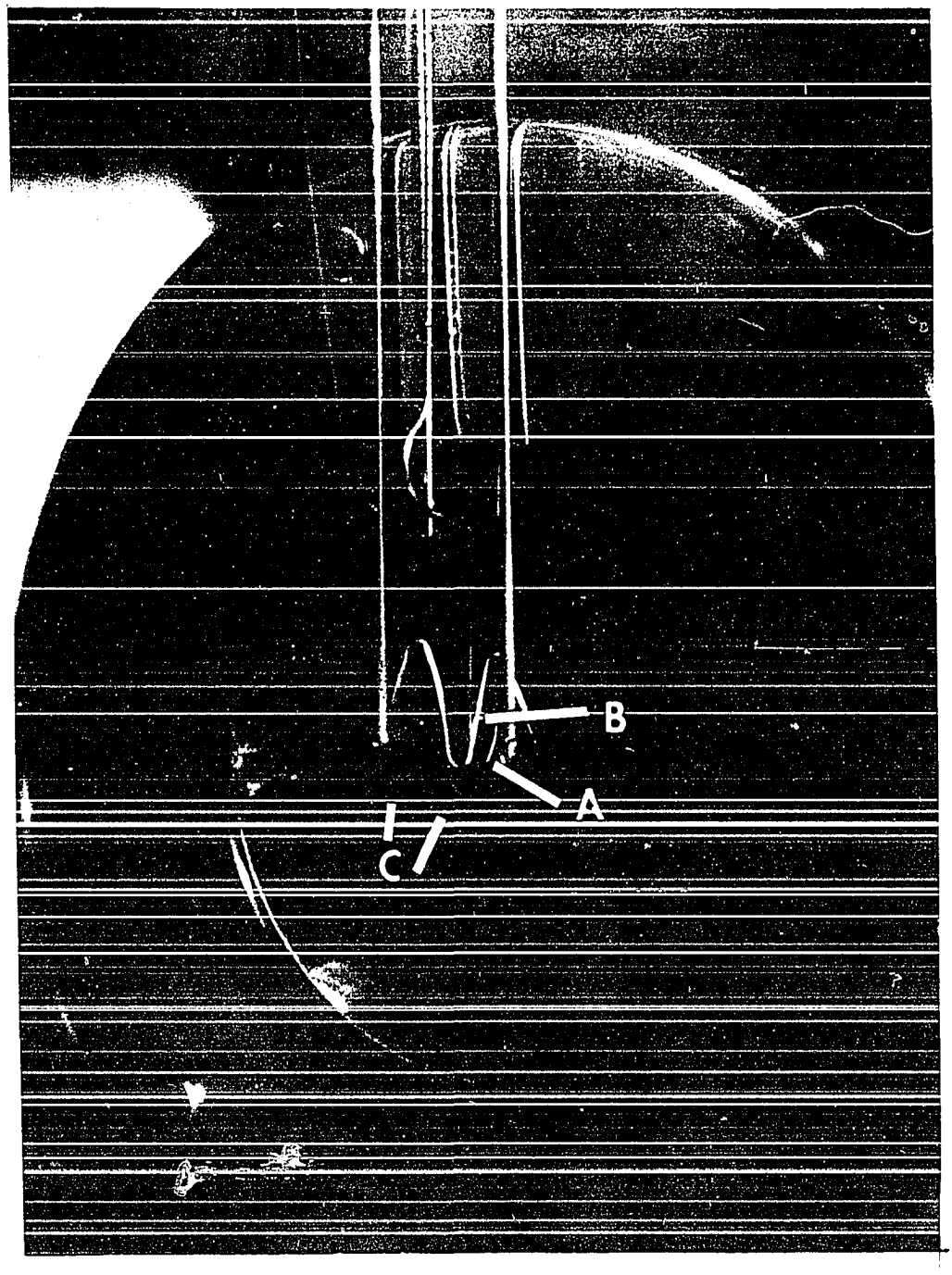

Fig. 3. Crystal holder assembly, a) crystal sample, b) emitter filament, c) thermocouple leads.

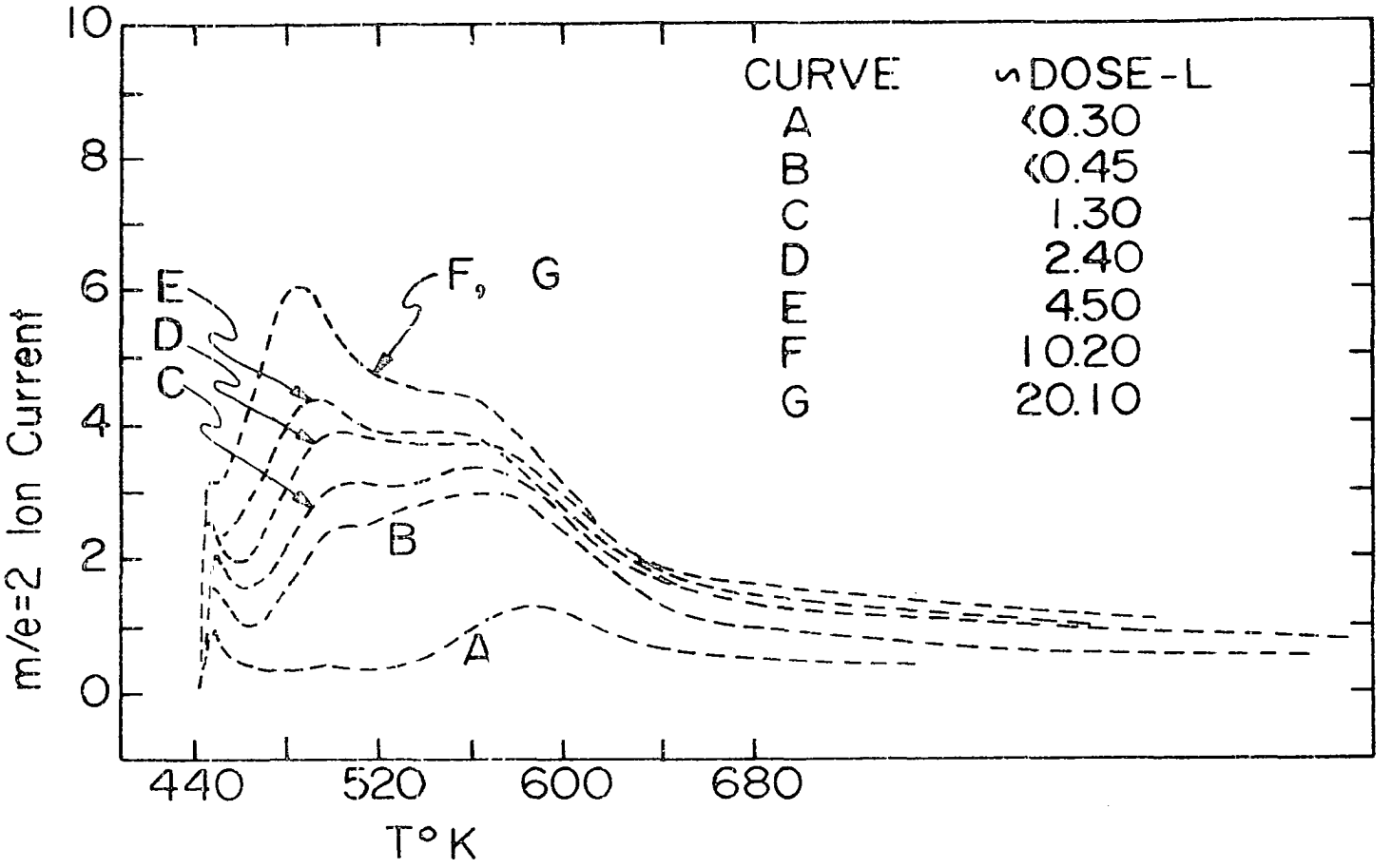

Fig. 4. Flash desorption of hydrogen from dosing of W(100) with H_2, i_2 ion current vs. temperature.

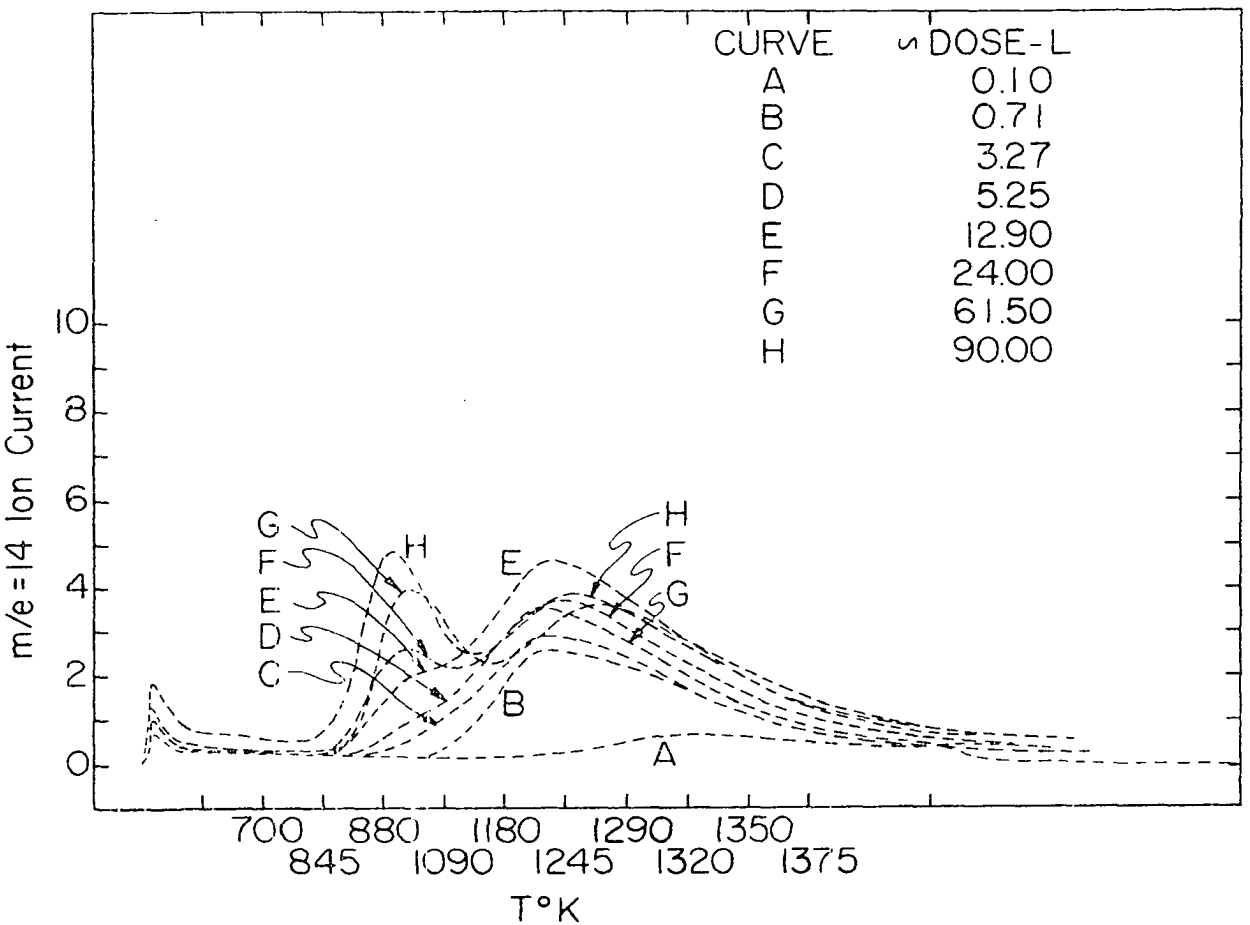

Fig. 5. Flash desorption of nitrogen from dosing of W(100) with N_2, i_{14} ion current vs. temperature, ion pump on during adsorption interval.

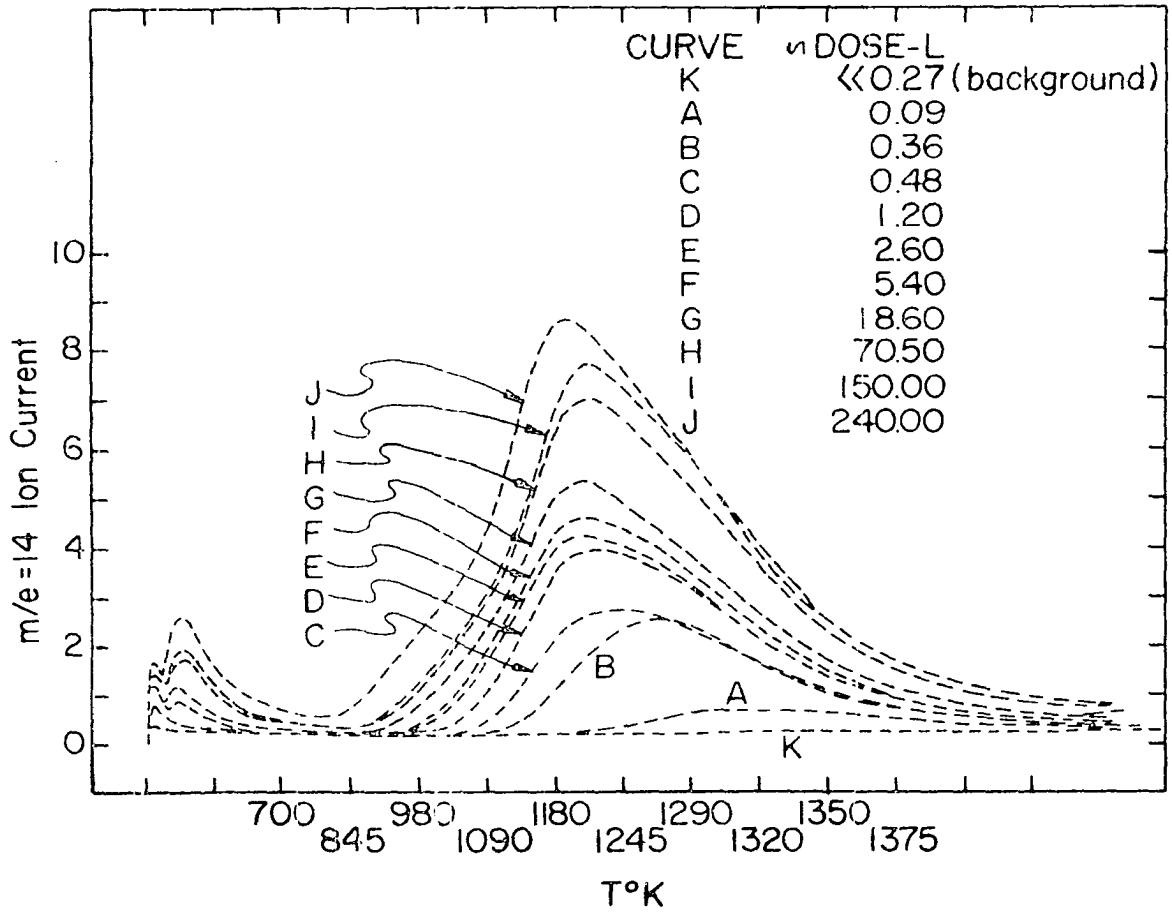

Fig. 6. Flash desorption of nitrogen from dosing of W(100) with N_2, i_{14} ion current vs. temperature, ion pump off during adsorption interval.

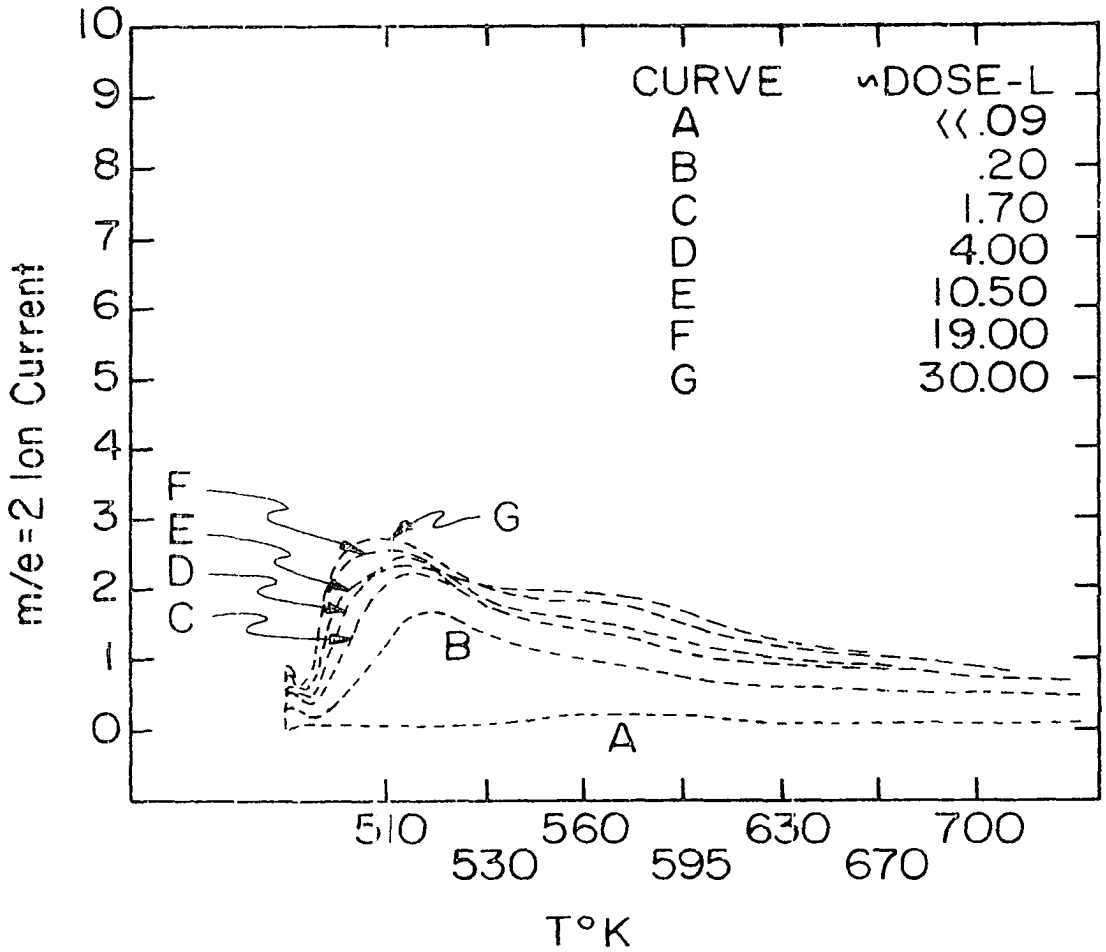

Fig. 7. Flash desorption of hydrogen from dosing of W(111) with H_2, i_2 ion current vs. temperature.

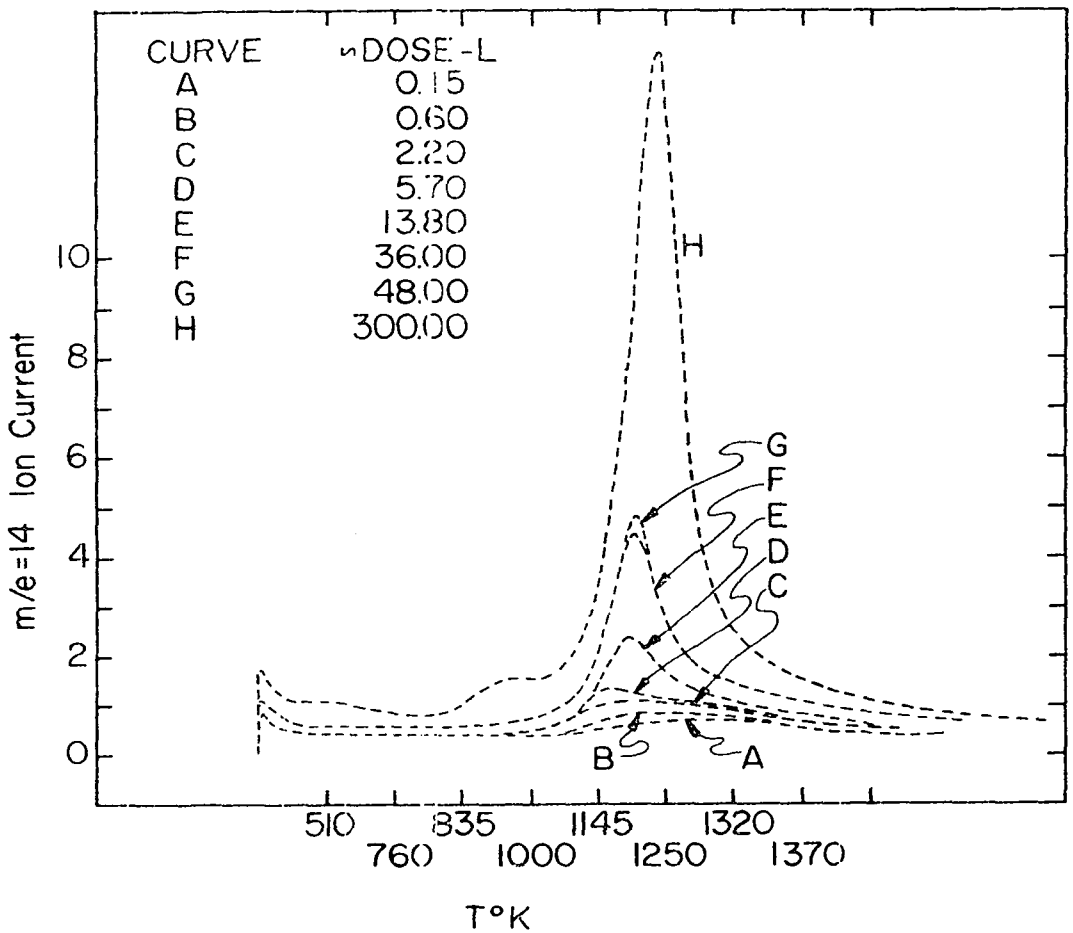

Fig. 8. Flash desorption of nitrogen from dosing of W(111) with N_2, i_{14} ion current vs. temperature.

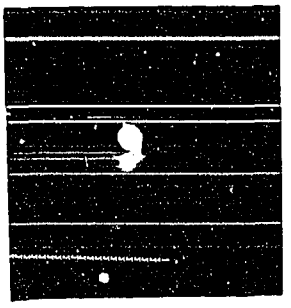

(a)

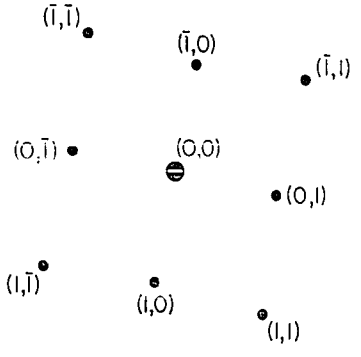

(b)

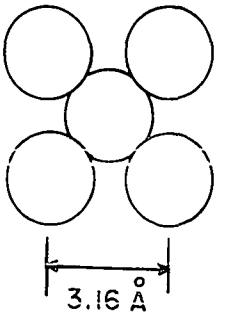

(c)

Fig. 9. LEED pattern, indexing and surface unit cell for W(100), a) LEED pattern from clean W(100) surface at 44eV. beam energy, b) indexing of beams shown in a), c) W(100) surface unit cell.

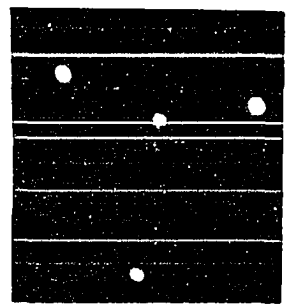

(a)

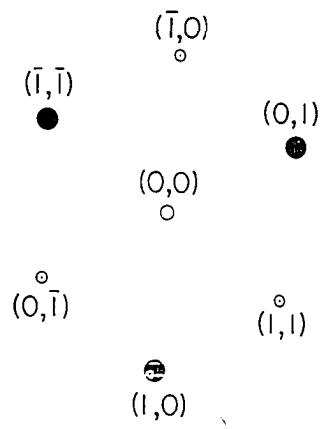

(b)

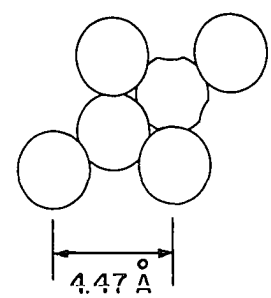

(c)

Fig. 10. LEED pattern, indexing and surface unit cell for W(111), a) LEED pattern from clean W(111) surface at 25 eV. beam energy, b) indexing of beams shown in a), c) W(111) surface unit cell.

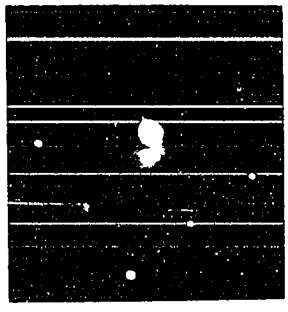

(a)

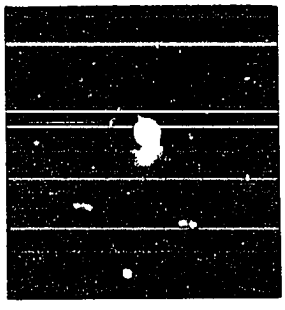

(b)

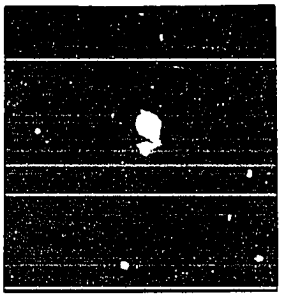

(c)

Fig. 11. LEED patterns resulting from the adsorption of H_2 on W(100) at 44 eV. beam energy, a) initial C(2 x 2) pattern, b) C(2 x 2) with split 1/2 order beams, c) (1 x 1) due to hydrogen saturated surface.

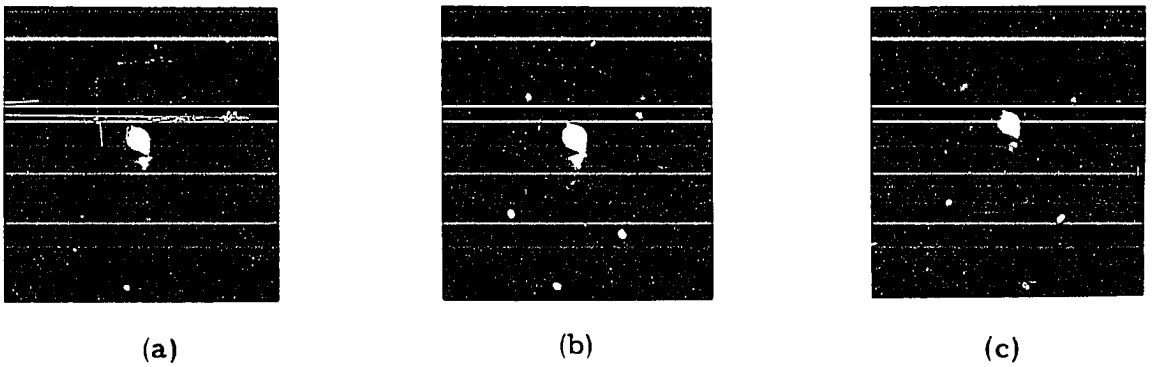

(a) (b) (c)

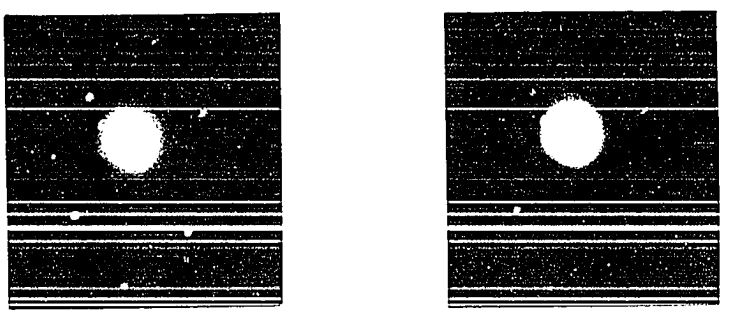

(d) (e)

Fig. 12. LEED patterns resulting from the interaction of N_2 with W(100), $P_{N_2} \sim 10^{-6}$ torr., 40 eV. beam energy, a) T = 700° K, b) T = 900° K, c) T = 1000° K, d) T = 1100° K, e) T = 1200° K.

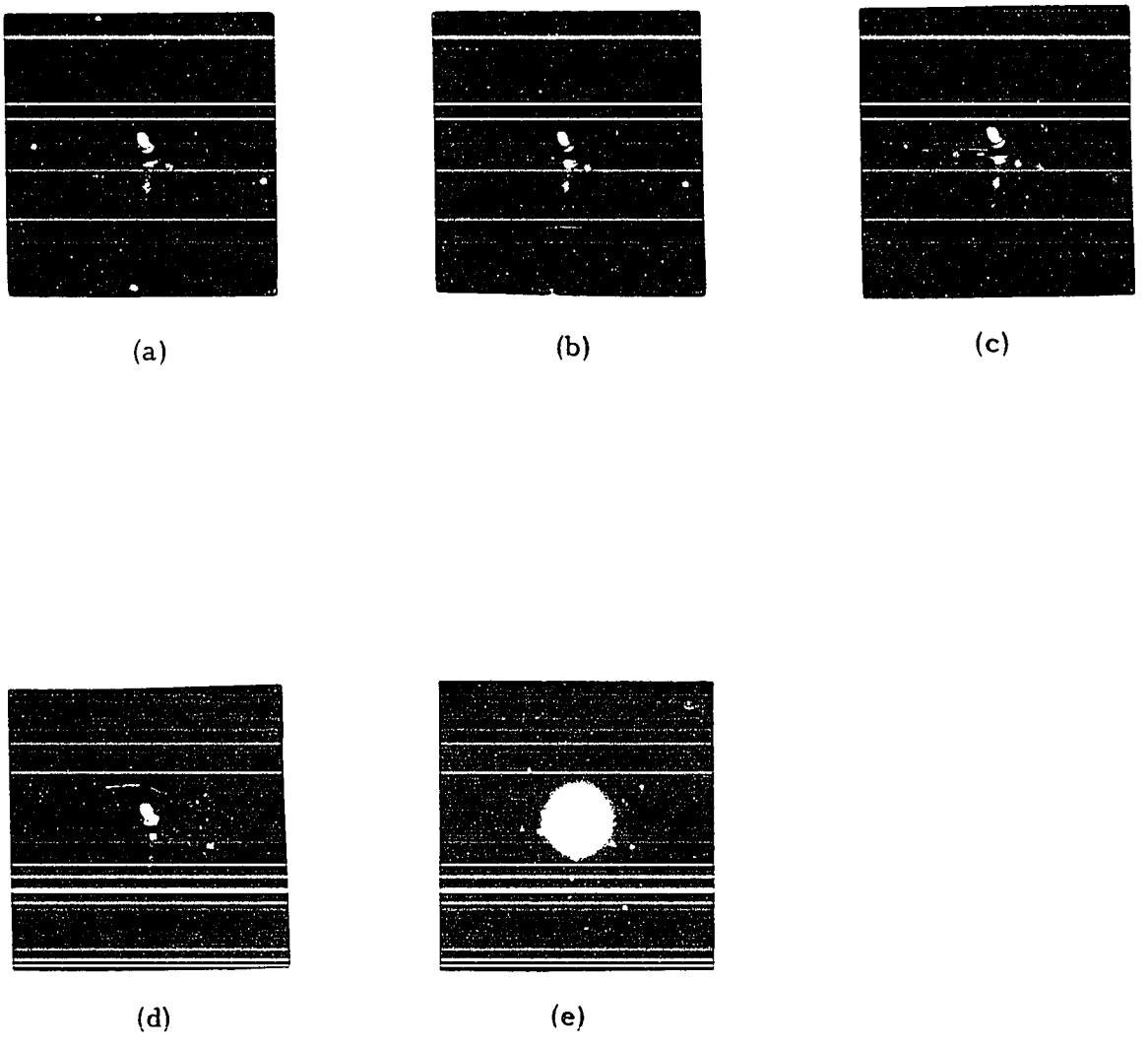

Fig. 13. LEED patterns resulting from the interaction of NH_3 with W(100), $P_{NH_3} \sim 10^{-6}$ torr., 40 eV. beam energy, a) T = 700° K, b) T = 800° K, c) T = 900° K, d) T = 1000° K, e) T = 1100° K.

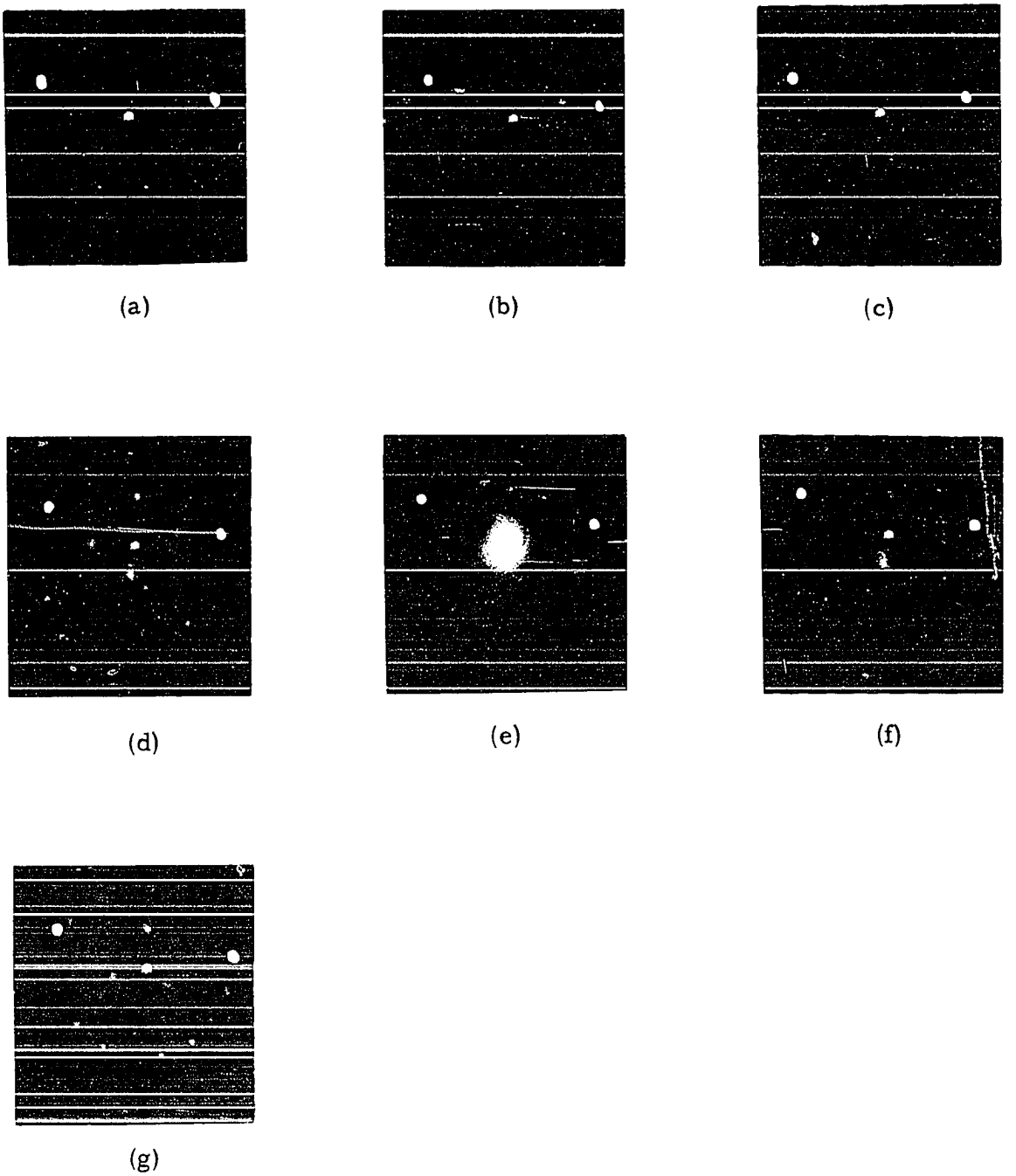

Fig. 14. LEED patterns resulting from the interaction of N_2 with W(111), $P_{N_2} \sim 10^{-5}$ torr., 25 eV. beam energy, a) T = 700°K, b) T = 800°K, c) T = 900°K, d) T = 1000°K, e) T = 1100°K, f) T = 1200°K, g) T = 1300°K.

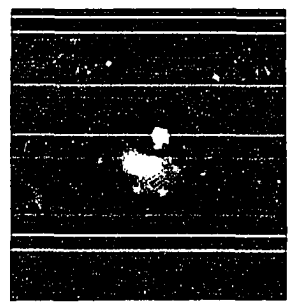

(a)

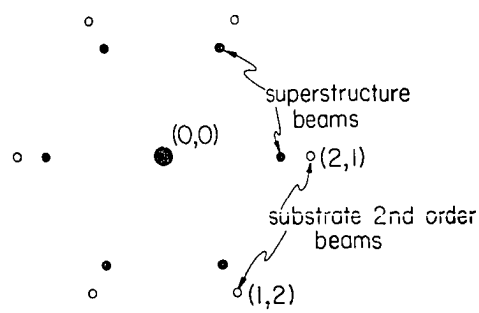

(b)

Fig. 15. LEED pattern and partial indexing due to surface structure formed on W(111) by NH_3 at $P_{NH_3} \sim 10^{-6} - 10^{-3}$ torr., $T \simeq 1000°K$, a) diffraction pattern at 55 eV. beam energy, b) partial indexing of pattern in a).

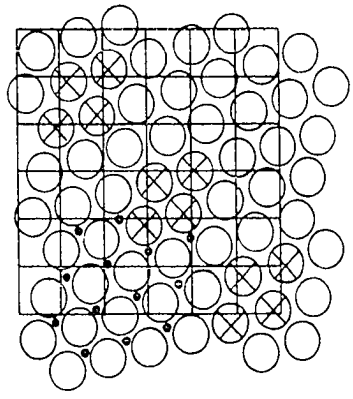

(a)

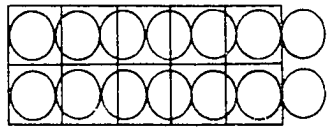

(b)

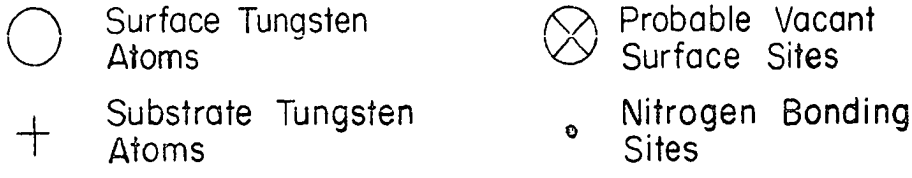

Fig. 16. Surface structures due to NH_3 interaction with W(100).
a) (6x6) superstructure unit cell formed at T = 1000°K. Square net of solid lines indicate substrate tungsten array,
b) (5x1) structure formed at T < 1000°K.

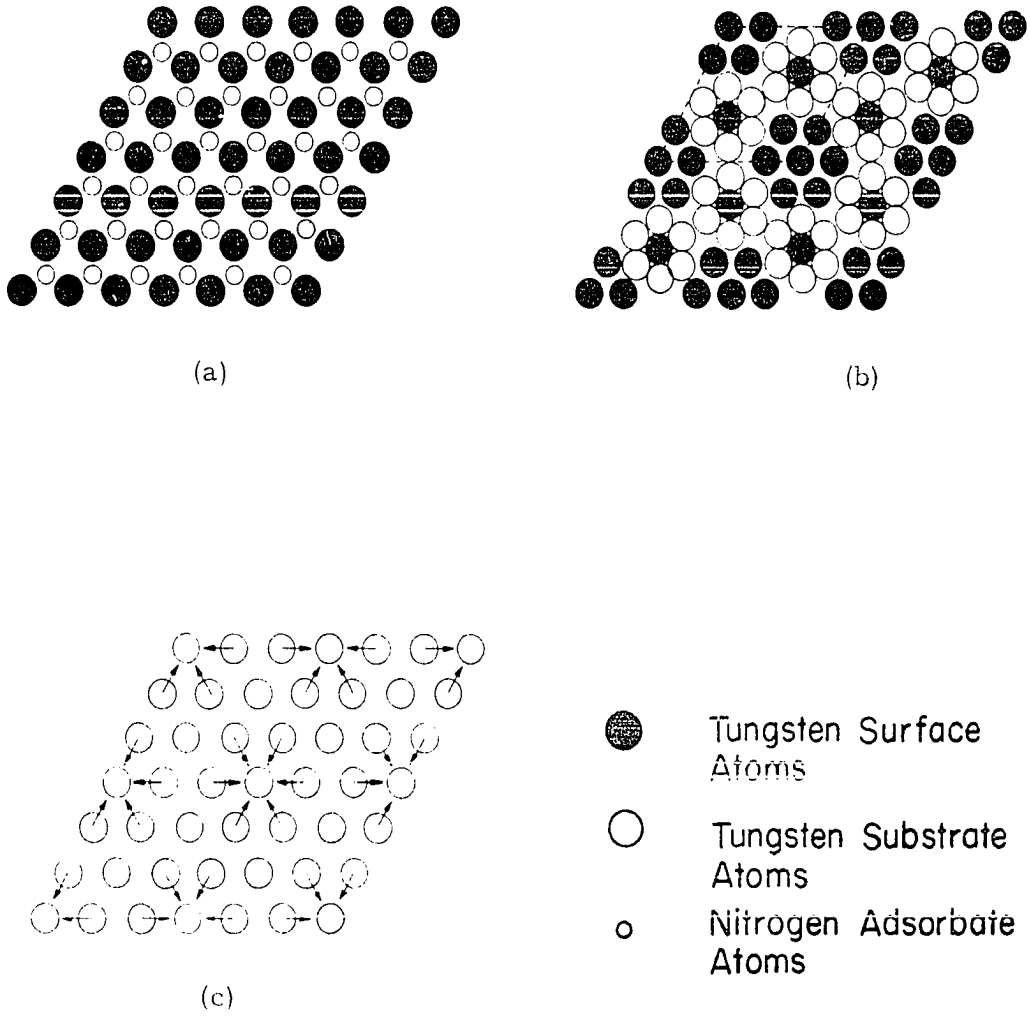

Fig. 17. Surface structures due to N_2 or NH_3 interaction with W(111). a) (1 x 1)-N array due to N_2 adsorption at $T \lesssim 900°K$, b) (3 x 3) structure due to N_2 or NH_3 interaction at $T \sim 1200°K$, c) W(111) surface array with arrows showing movement of atoms to form (3 x 3).

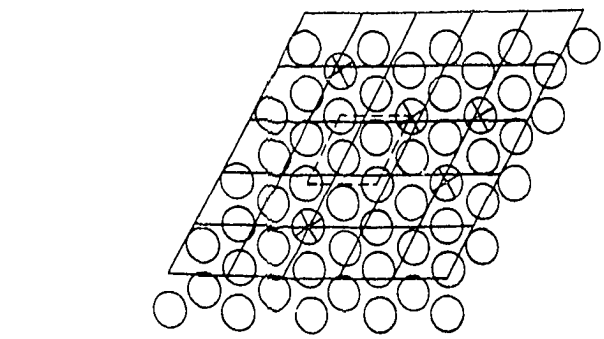

○ -Tungsten Surface Atoms

⊗-Probable Vacant Surface Sites

⟋ -Tungsten Substrate Atoms

Fig. 18. (5 x 5) superstructure unit cell due to NH_3 interaction with W(111) at T ~ 1000°K. Solid lines represent substrate (111) array. Dashed lines represent triply primitive unit cell of surface structure.

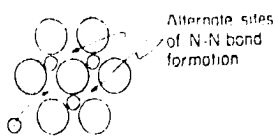

○ -Tungsten Surface Atom

o - Nitrogen Atom

Fig. 19. Hexagonal unit of tungsten surface atoms showing positions of bound nitrogens and sites of N-N bond formation leading to molecular desorption of N_2. Dashed arrow indicates addition of nitrogen atom to cell resulting in a transition state stoichiometry of $W_{7/3}N_3$.